Renewable and Sustainable Energy Reviews 151 (2021) 111525

Contents lists available at ScienceDirect

Renewable and Sustainable Energy Reviews

journal homepage: www.elsevier.com/locate/rser

A synthesis of feasible control methods for floating offshore wind turbine system dynamics

Kamran Ali Shah [a], Fantai Meng [a], Ye Li [a,e,f,g,*], Ryozo Nagamune [b], Yarong Zhou [a], Zhengru Ren [d], Zhiyu Jiang [c]

[a] Multi-function Towing Tank, State Key Laboratory of Ocean Engineering, School of Naval Architecture, Ocean & Civil Engineering, Shanghai Jiao Tong University, Shanghai 200240, China
[b] Department of Mechanical Engineering, The University of British Columbia, Vancouver, BC, Canada V6T1Z4
[c] Department of Engineering Sciences, University of Agder, NO 4879, Grimstad, Norway
[d] Department of Marine Technology, Norwegian University of Science and Technology, NO 7491, Trondheim, Norway
[e] School of Energy and Power Engineering, Lanzhou University of Technology, 730050, Lanzhou, China
[f] Gansu Provincial Technology Centre for Wind Turbines, 730050, Lanzhou, China
[g] MOE Key Laboratory of Hydrodynamics, Shanghai Jiaotong University, 200240, Shanghai, China

ARTICLE INFO

Keywords:
Floating offshore wind turbines
Wind turbine control
System dynamics
Wind power
Cost reduction
Floating platforms

ABSTRACT

During the past decade, the development of offshore wind energy has transitioned from near shore with shallow water to offshore middle-depth water regions. Consequently, the energy conversion technology has shifted from bottom-fixed wind turbines to floating offshore wind turbines. Floating offshore wind turbines are considered more suitable, but their cost is still very high. One of the main reasons for this is that the system dynamics control method is not well-adapted, thereby affecting the performance and reliability of the wind turbine system. The additional motion of the platform tends to compromise the system's performance in terms of power maximization, power regulation, and load mitigation. To provide a recommendation based on the advantages and disadvantages of different control methods, we systematically analyze feasible control methods for existing floating offshore wind turbine designs. Based on a brief overview of floating offshore wind turbine system dynamics, we present several promising control methods by classifying them as blade-pitch-based and mass–spring–damper-based. Furthermore, we emphasize on the incoming wind and wave forecasting associated with the control methods. We then compare different methods by evaluating a matrix involving platform motion minimization, load mitigation, and power regulation and identify the advantages and disadvantages. Finally, recommendations and suggestions for further research are provided by integrating the advantageous control algorithm and forecasting technologies to reduce costs.

1. Introduction

Wind energy is one of the leading commercial renewable energy resources, and it has significant potential in both onshore and offshore areas [1,2]. Over the last decade, there has been a rapid increase in global (onshore and offshore) wind power production, as shown in Fig. 1; the total installed capacity for onshore wind turbines has increased from 159 to 651 GW. In particular, a record increase in the annual installed offshore wind energy capacity was reported in 2019. The new annual offshore installed capacity is estimated to exceed 30 GW by 2030, with a compound annual growth rate of 18.6% for the first half and 8.2% during the latter half of the decade (Fig. 2).

1.1. Outlook on offshore wind

Offshore wind quality is superior to onshore wind quality, because offshore wind blows more consistently with a higher annual average speed [3,4]. The majority of the offshore wind potential is distributed over areas of water with a depth of more than 60 m, and the percentage of this resource is up to 80% in Europe [5]. Therefore, there is a need to develop offshore wind turbines in the ocean. Furthermore, the offshore wind potential is expected to ease the transition toward renewable energy resources and maintain the increase in the global temperature at 1.5 degrees Celsius, according to the recommendation of the Intergovernmental Panel on Climate Change [6]. Additionally, the

* Corresponding author at: Multi-function Towing Tank, State Key Laboratory of Ocean Engineering, School of Naval Architecture, Ocean & Civil Engineering, Shanghai Jiao Tong University, Shanghai 200240, China.
E-mail address: ye.li@sjtu.edu.cn (Y. Li).

https://doi.org/10.1016/j.rser.2021.111525
Received 12 May 2020; Received in revised form 1 July 2021; Accepted 19 July 2021
Available online 25 August 2021
1364-0321/

Nomenclature

ANFIS	Adaptive Neuro-Fuzzy Inference System
ANN	Artificial Neural Network
AR	Auto-Regressive
ARIMA	Auto-Regressive Integral Moving Average
ARMA	Auto-Regressive Moving Average
BEM	Blade Element Momentum
CBP	Collective Blade Pitch
CBPC	Collective Blade Pitch Control
CNN	Convolutional Neural Network
DOF	Degree of freedom
DAC	Disturbance Accommodating Control
DMD	Dynamic Mode Decomposition
EMD	Ensemble Mode Decomposition
ESPRIT	Estimation of Signal Parameters via Rotational Invariance Techniques
ELM	Extreme Learning Machine
FAST	Fatigue Aerodynamics Structures and Turbulence
FF	Feedforward
FOWT	Floating Offshore Wind Turbine
GSPI	Gain-Scheduled Proportional–Integral
GP	Gaussian Process
HAR	Hammerstein Auto-Regressive
HAWC2	Horizontal Axis Wind Turbine Code-Second generation
HAWT	Horizontal Axis Wind Turbine
HMD	Hybrid Mass Damper
IBP	Individual Blade Pitch
IBPC	Individual Blade Pitch Control
IPCC	Intergovernmental Panel's recommendation on Climate Change
LSSVM	Least Square Vector Support Machine
LCOE	Levelized Cost of Energy
LIDAR	Light detection and ranging
LPV	Linear Parameter Varying
LQR	Linear Quadratic Regulator
MLC	Machine learning control
MPC	Model Predictive Control
NMPC	Nonlinear Model Predictive Control
MBS	Multi-Body System
MIMO	Multi-Input Multi-Output
NREL	National Renewable Energy Lab
PI	Proportional–Integral
RNN	Recurrent Neural Network
SISO	Single-Input Single-Output
SINDy	Sparse Identification of Nonlinear Dynamics
SMC	Sliding Mode Control
SC	Structural Control
SVM	Support Vector Machine
TRL	Technology Readiness Level
TLP	Tension leg platform
TMD	Tune Mass Damper
TLD	Tuned Liquid Damper
VAWT	Vertical axis wind turbine

environmental hazards caused by land-based wind farms, such as visual and noise impacts [7–9], and the lower-quality onshore wind may be avoided by installing wind turbines in offshore regions.

Offshore wind turbines face a significant challenge of high levelized cost of electricity (LCOE). Unlike existing energy resources, offshore wind technology is in the pre-commercial stage so that there is still room to reduce the LCOE. It is known that the method to lower the LCOE is to either reduce the total cost or improve the energy production. Therefore, one can say that an optimal design with an appropriate control approach is the solution to address all these challenges. Technically, offshore wind turbines can be categorized as bottom-fixed offshore wind turbines and floating offshore wind turbines (FOWTs), based on the design of their substructures. Bottom-fixed wind turbines are not suggested for wind turbines operating in the ocean, because economic constraints hinder the development of a bottom-fixed support structure for wind turbines operating beyond 60 m water depth. Because the LCOE of a bottom-fixed offshore wind turbine increases significantly as the water depth increases, the FOWT becomes an optimal solution under the cost–benefit trade-off.

1.2. FOWT system dynamics

For the design of the FOWT system, it is believed that placing a wind turbine on top of a floating platform is a feasible solution for operating in the ocean. The major parts of an FOWT system are (1) a wind turbine to harvest energy from the wind, (2) a floating platform support, and (3) mooring lines to provide the wind turbine structure support in terms of orientation and position, as well as platform support (Fig. 3). There are two types of wind turbines that may be used to generate wind energy: horizontal-axis wind turbines (HAWTs) and vertical-axis wind turbines (VAWTs) [12]. In this study, as the VAWT is not our focus, we only consider the HAWT. Readers interested in VAWTs and FOWTs with VAWT are referred to [13].

The performance of an FOWT system can be significantly compromised by the motion of the floating platform caused by the environmental loads. This is not only caused by the extreme wave condition [14], but also a combination of wind, wave and current [15]. An unstable platform may decrease the nominal wind turbine area and affect energy generation. Platform motion may also increase tower loads compared to fixed-bottom wind turbines and negatively impact the structural life of the system, which then requires extensive maintenance down time [16]. Consequently, it increases the operational and maintenance cost [17] and thus the overall LCOE compared against with other offshore renewables [18].

To mitigate these environmental impact, control methods are quite often used. During the past decade, numerous controllers have been designed to address the shortcomings of floating platforms using a range of controllers, such as proportional–integral (PI) [19–22], linear quadratic regulator (LQR) [23–25], linear parameter varying (LPV) [26], and model predictive control (MPC) [27–31]. They are benefited from the experiences in the traditional offshore applications such as ships [32], underwater vehicles [33], and standard offshore platform [34] and bottom-fixed wind turbine control [35]. These control algorithms utilize the blade pitch mechanism by actuating blades identically (collective blade pitch) or separately (individual blade pitch) to provide the wind turbine with aerodynamic thrust to suppress platform motion and maximize power generation and load mitigation. In comparison, mass–spring–damper-based FOWT control methods introduce an extra degree of freedom and decouple the pitching mechanism by providing the required thrust to reduce pitching phenomena [36]. Improved control mechanisms may elevate the performance of FOWTs, leading to a reduction in the LCOE. However, the LCOE of FOWTs is still higher than that of the bottom-fixed wind turbines.

The performance of advanced controllers can be improved by incorporating wind and wave forecasting techniques. Predicted wind and wave information ahead of their encounter with the wind turbine can provide preview-based advanced controllers with sufficient time to respond to incoming disturbances and orient wind turbines for optimal performance. The wind turbine industry has already benefited

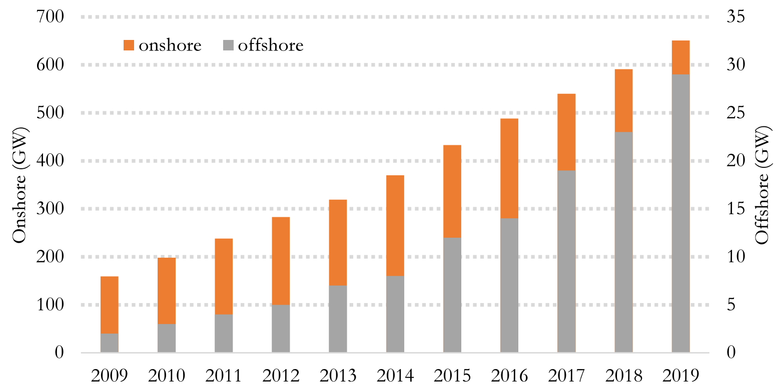

Fig. 1. Global cumulative installed (onshore and offshore) wind energy capacity.
Source: Data obtained from [10].

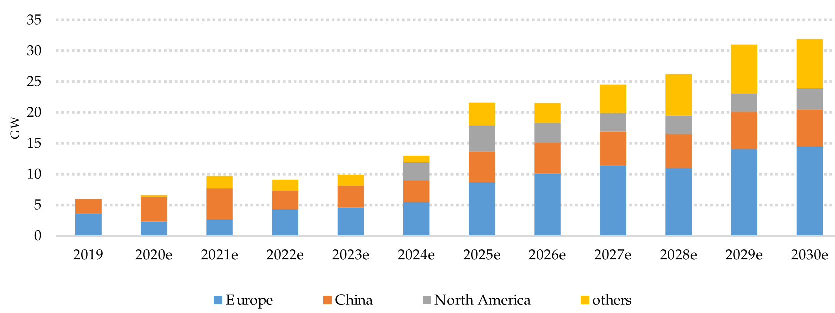

Fig. 2. New annual installation prediction until 2030.
Source: Data obtained from [11].

from wind forecasting for wind farm planning, operation, and grid integration [37]. Numerous forecasting techniques for wind [38,39], current [40] and wave [41,42] have been presented in the literature, ranging from long-term (three days to one week or more) to short-term (a few seconds to 30 min) prediction horizons [43–47]. However, the controller response time for FOWTs is in the short-term prediction horizon category [48,49]. Compared with traditional feedback controllers, advanced controllers based on light detection and ranging (LIDAR) information [27] incorporate the incident wind disturbance before reaching the wind turbine, thus enhancing the performance. An accurate short-term disturbance prediction incorporated in modern control systems, such as feedforward control or MPC, can enhance the performance in terms of platform stability and loading and deal with the incident disturbance better than the counterpart feedback controllers, resulting in further lowering of the LCOE.

1.3. Objective

It is clear that, as the design of an FOWT system is not a single solution, the control approaches associated with the design become even more complicated to define. However, one must select an appropriate control approach for a certain design. Therefore, we decided to conduct a comprehensive review of the state-of-the-art in FOWT control and highlight potential improvements to lower the LCOE with the use of incident wind and wave forecasting, and we summarize the effort in this paper. It is worth noting that because the number of FOWTs in the operational stage is limited, we studied several methods in the conceptual stage. That is why we refer to “feasible control methods” in the title of this paper.

The remainder of this paper is organized as follows. Section 2 provides a brief overview of the FOWT system dynamics and the overall framework of the control system. Then, a systematic review of the control methods is presented in Section 3. Section 4 details the wind and wave forecasting techniques for the control system. We comprehensively discuss the advantages and disadvantages of different control algorithms with respect to the platform design in Section 5. Finally, the conclusion of this review and recommendations for possible control methods for future FOWT designs are given in Section 6.

2. System description

Before discussing the details of the control methods and algorithm, we review the system dynamics of the FOWT for those readers who are not very familiar with it.

2.1. Overview of system dynamics

The concept of operating wind turbines using a floating platform in the ocean is based on the existing employment of floating platforms for oil and gas exploration in the ocean [50]. Several concepts have been proposed to achieve platform stability for FOWTs such as barges, tension leg platforms (TLPs), spar-buoys, and semi-submersibles [51], as shown in Fig. 4. These concepts include buoyancy-stabilized platforms, mooring line-stabilized platforms, and ballast-stabilized platforms. Buoyancy-stabilized platforms use submerged body volume to achieve stability, for example, barges and semi-submersible platforms. The TLP is a typical example of a mooring line-stabilized platform. In contrast, the spar-buoy is an example of a ballast-stabilized platform that benefits from the heavy ballasting of the bottom of the platform to stabilize the structure. A qualitative comparison between the associated properties of existing floating platforms is presented in Table 1.

Floating platforms introduce additional loading (hydrodynamic loading and mooring loading) owing to incident waves, as well as aerodynamic loading on the wind turbine, regardless of the attachment

Table 1
Properties of floating platforms.

Platform	Stability	Operational at the water depth (m)	Motions	Draft	Fabrication Cost and Installation
Barge	Hydrostatic	50	High	Small	Low/Easy
Spar-buoy	Ballast	150	Low	Large	Average/Challenging
Tension leg	Mooring	50	Average	Small	Average/Challenging
Semi-Submersible	Hydrostatic	50	High	Small	Large/Easy

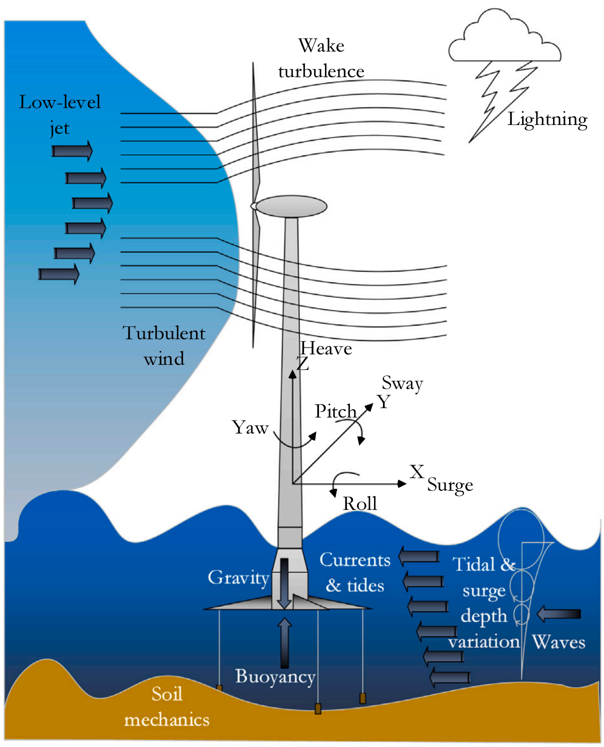

Fig. 3. FOWT operating in the sea.

to the sea bottom with mooring lines. Wind energy generation based on aerodynamic wind loads is reported in Appendix A. The incident-wave-associated FOWT loading leads to an additional six degree-of-freedom (DOF) motion compared to bottom-fixed wind turbines, as shown in Fig. 3, and an FOWT is stabilized using a TLP base. The stability of the floating platform is one of the dominant concerns of FOWT technology, and it may directly impact the performance and safety of FOWTs, leading to increased cost [52]. The performance and operation of the wind turbine are coupled with the platform motion. Therefore, it is essential to minimize the platform motion during FOWT operation. Please note that we use the TLP type of FOWT as an example in Fig. 3 to explain the working principle with minimum drawing effort; this does not imply that we have a preference for it over the other designs, and the same philosophy applies to the rest of the paper as well, such as the figures in Appendix B.

The operational range of a wind turbine is divided into three operating regions (ORs) based on the incoming wind speed, as shown in Fig. 5. In region I, the wind speed is less than the cut-in wind speed ($V_{\text{cut-in}}$), and the wind turbine is in a parked condition. In region II, the wind speed value is less than the rated value (V_{Rated}). The control objective focuses on the maximum energy extraction from the wind by maintaining the blade pitch at an optimal angle. In region III, where the wind speed value surpasses V_{Rated}, the objective shifts toward regulating the generated power with pitch angle activity. When the wind speed reaches the cut-off wind speed ($V_{\text{cut-off}}$), mechanical brakes are applied to ensure the safety of the wind turbine. In the case of FOWTs, the number of control objectives becomes more complex with additional platform motions. For an FOWT, the floating platform, regardless of being tied to the seabed, may experience significant platform stability issues due to incident waves and wind loads.

2.2. Framework of FOWT control systems

FOWTs are prone to platform motion owing to the floating base, leading to performance deterioration. However, an effective control system can deal with platform motion and achieve optimal wind energy generation. Existing control mechanisms for bottom-fixed wind turbines are rendered infeasible for FOWTs, owing to the additional platform motion of the FOWT. However, bottom-fixed wind turbine controllers can be modified to include the platform motion suppression objective.

The majority of FOWT controllers are based on feedback control mechanisms. These feedback controllers mainly respond to the incident wind and wave disturbance after the disturbance interacts with the wind turbine system. Advanced preview-enabled controllers have been presented in the literature. Preview-enabled controllers orient wind turbines ahead of the incoming disturbance, thereby increasing the performance. Such controllers can be used to minimize the effect of incoming disturbances better than feedback controllers by using a prediction mechanism for both the incoming wind and wave. The benefit of the feedforward mechanism may be further extrapolated by using incident wind and wave prediction to improve the controller performance, as shown in Fig. 6.

3. FOWT control structure

The control system of a wind turbine is responsible for handling the aerodynamic wind load and converting wind energy into electric power. In general, there are multiple control levels to deal with wind turbine operations. The primary-level supervisory control deals with the startup and shutdown of the wind turbine. The wind turbine starts generating power when the wind speed is greater than $V_{\text{cut-in}}$, and shutdown is triggered in the presence of excessive wind beyond $V_{\text{cut-off}}$, as it may harm the wind turbine structure. The second-level operational control is dedicated to achieving control objectives based on the wind turbine operating region, as shown in Fig. 5. The third-level control is concerned with yaw and pitch actuation systems and related electronic units. The scope of this study was limited to the second-level operational control of a wind turbine. In this section, the control objectives and methodologies used to achieve these objectives for FOWTs are discussed in detail.

3.1. Control objectives

The control objectives of a wind turbine vary based on the operating regions, namely, maximum power generation operating in region II and power regulation in III, as shown in Fig. 5. There are generally two control loops to achieve these control objectives, as shown in Fig. 7. In region II, the torque control loop of the wind turbine is used to maximize the generated power by operating near the optimal C_p by using a fixed blade pitch angle to an optimal value, based on Eq. (1). In region III, the objective shifts toward regulating the generated power at the rated value. The blade pitch control loop regulates the aerodynamic loads and power generated by manipulating the blade pitch. There are two standard pitching strategies for the region III pitch control loop:

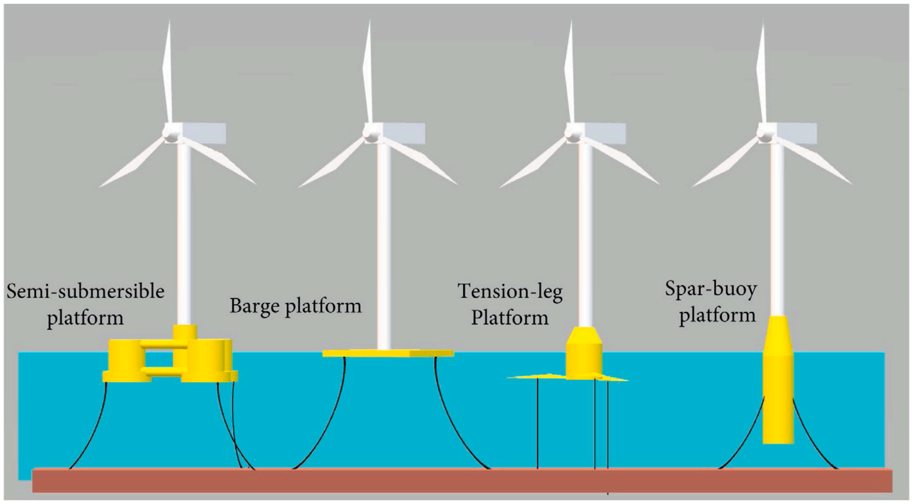

Fig. 4. FOWT platforms (semi-submersible platform, barge, tension-leg, and spar-buoy).

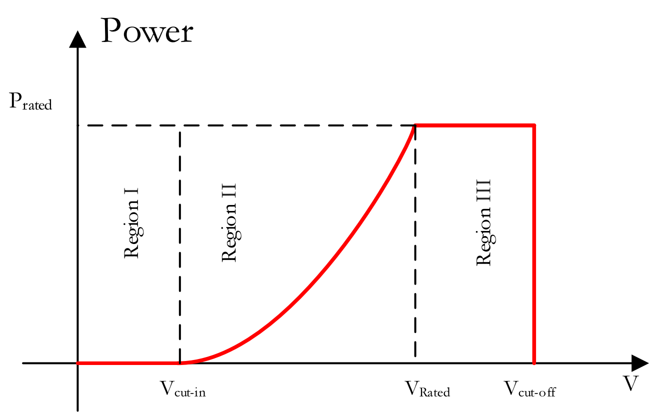

Fig. 5. Operating regions of a wind turbine.

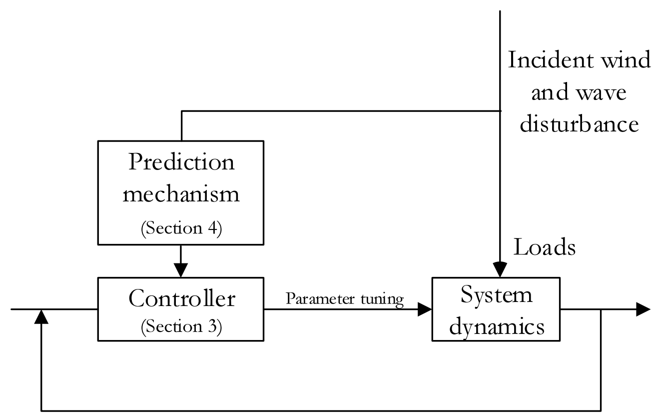

Fig. 6. FOWT control framework.

pitch-to-stall and pitch-to-feather [53]. The generator torque control includes two ways to regulate power while operating in region III: constant torque and constant power, based on the relationship in (2). In the constant-torque mechanism, the generator torque is fixed to the rated torque, and the generator speed is regulated using the blade pitch angle. In constant-power control, the generator torque and blade pitch angle are simultaneously manipulated. The constant-torque methodology is simpler in terms of reduced loads on wind turbines; however, the power quality is affected. By contrast, the constant-power methodology improves the power quality but increases the controller complexity and wind turbine loads [23].

However, the major problem associated with FOWT occurs because of platform motion during operation in region III. The wind turbine structure undergoes undesired pitching phenomena, often called negative damping [54]. The frequency of the platform is coupled with the blade pitch mechanism while operating in region III, causing a surge in the pitching motion of the platform, leading to problems such as poor power quality and increased loads. Therefore, an adequate control mechanism is required to achieve the standard wind turbine control objectives and deal with the platform pitching phenomena associated with the FOWT floating platform.

$$T_{gen} = \frac{\pi \rho R^5 C_{p,\max}}{2\lambda_o^2 N^3}\omega_{gen}^2 = K\omega_{gen}^2 \tag{1}$$

$$T_{gen} = \frac{P_{rated}}{\eta_{gen}\omega_{gen}} \tag{2}$$

where

- T_{gen} = Generator torque
- ρ = Air density
- R = Rotor radius
- N = Gear box ratio
- $C_{p,\max}$ = Maximum power coefficient
- λ_o = Tip speed ratio related to $C_{p,\max}$
- ω_{gen} = Generator rotational speed
- η_{gen} = Generator efficiency
- P_{rated} = Rated generated power

Several system models have been proposed in the literature, to develop control schemes for FOWT and preview the outcome without running the actual wind turbines. Appendix B provides the details of these simulation codes for the readers interested in FOWT system models.

3.2. Control methodologies

Control methodologies for FOWTs designed to deal with undesired platform-associated motions can be divided into two categories: (1) blade pitch-based FOWT control methods and (2) mass–spring–damper-based FOWT control methods. In the former, existing control variables such as blade pitch angle, generator torque, and yaw angle of a wind turbine are used to achieve region-based control objectives and platform motion suppression. Yaw control is beyond the scope of this study, as the wind is assumed to be unidirectional for the control

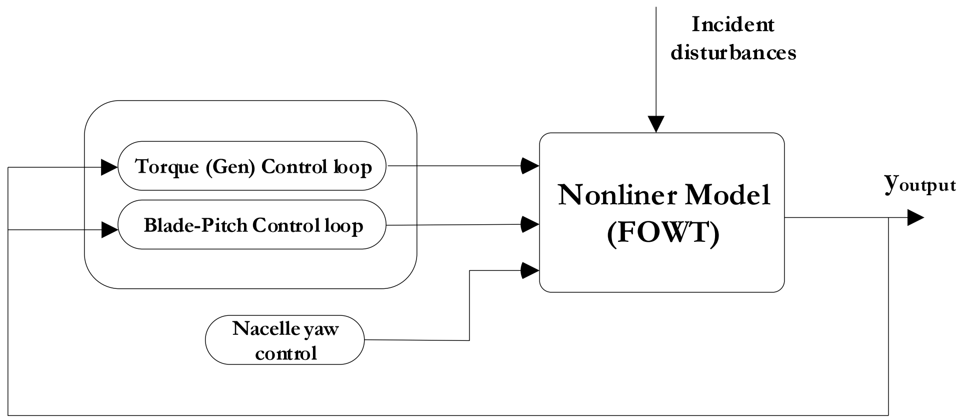

Fig. 7. Wind turbine standard control loops.

methodologies under consideration. In the latter category, additional DOFs are introduced into the system to deal with the platform stability and associated problems of FOWTs.

This section provides a discussion on the range of blade-pitch and mass–spring–damper-based control methods reported in the literature.

3.2.1. Blade-pitch based FOWT control methods

The majority of FOWT control methodologies use a blade pitch actuator to achieve wind turbine platform stability. These methodologies can be further divided into two subcategories: conventional and advanced FOWT control methods.

3.2.1.1. Conventional FOWT control methods. Conventional FOWT controllers are simple and easily designed control mechanisms based on the single-input single-output (SISO) principle. Independent control loops are applied in parallel to achieve multiple control objectives, as shown in Fig. 7.

The platform pitching motion of the FOWT was minimized by keeping the frequency of the blade pitch mechanism lower than the resonance frequency of the platform by Larsen et al. [19]. For region II, a variable-speed control loop was used to maximize the generated power. A region of constant speed was introduced between regions 2 and 3, followed by a constant-torque loop in region III. The pitching action was determined by a gain-scheduled proportional–integral (GSPI) controller for region III. Improved platform pitching was achieved using a less aggressive control methodology at the cost of reduced power quality and poor rotor speed regulation.

Another GSPI controller-based solution for the negative platform damping problem of the barge-based FOWT was provided by Jonkman [20]. Two independent SISO controls were designed: a generator-torque controller to generate maximum power in region II and maintain the power captured at the rated value in region III. A GSPI controller was used to adjust the rotor speed as a function of blade pitch activity based on the collective blade pitch (CBP). Jonkman et al. [20] designed additional control loops upon facing complications regarding platform oscillations and power fluctuations during the early design synthesis. Tower-top feedback control, active pitch-to-stall control, and a controller based on detuned gains were the additional loops included in the original design mechanism. These additional loops were proposed to minimize the Fore–aft motion of the tower, instability of the platform yaw, and excessive barge motions. The tower-top feedback control failed to improve the pitching motion of the platform. Furthermore, active pitch-to-stall control was found to be suitable for power regulation for the barge platform, at the expense of increased platform pitching motion. However, detuned gains proved to be the most suitable controller, as it reduced the blade activity and addressed the platform pitching issue. This configuration is used for testing newly designed controllers and is considered as the baseline FOWT control [55].

The baseline controller designed by Jonkman et al. [20] was analyzed for different platforms by Matha et al. [56]. The TLP, barge, and spar-buoy floating concepts were compared in terms of fatigue loads and platform stability. Matha et al. [56] modified the baseline controller for a spar-buoy platform. Constant-torque control was designed to improve the platform pitching motion while operating in region III, in contrast to the constant-power controller originally designed by Jonkman et al. [20]. Meanwhile, the controller's bandwidth was kept low to avoid coupling with the frequency of the platform. It was noticed that the barge platform is cost-effective, but its inability to withstand incident loads may cause stability issues. The spar-buoy platform showed resistance toward tower loading compared to the barge platform. However, the deployment of the spar-buoy platform is costly because of its intricate design and assembly. In comparison, TLP was found to have better performance among the compared concepts. However, it was found that the anchoring system of the TLP may increase the cost.

Platform instability was addressed by using the pitching velocity as an input to regulate the generator rated speed in region III [21]. The generator speed was used to provide counter thrust to suppress the platform pitch motion and achieve platform stability. This unique control methodology reduced the negative damping and blade pitch activity at the cost of acceptable rotor speed fluctuations and power variations.

A control strategy based on the estimation of wind speed to suppress the negative damping of the Hywind concept platform [54] was proposed by Skaare et al. [22]. This control mechanism improved tower loading and nacelle oscillations. Simultaneously, poor rotor speed regulation and reduced power generation were observed compared to the conventional blade pitch mechanism. Moreover, because the strategy was based on the estimated form of wind in region III, the effectiveness of this control scheme was mainly governed by the wind estimation quality.

SISO-based conventional controllers borrowed from bottom-fixed wind turbine systems are a reasonable starting point for FOWT control. However, as suggested by Jonkman [20], multiple-input multiple-output (MIMO) state-space control methods for FOWT may improve the performance further with a superior approach to deal with the cross-coupling of control loops and disturbances.

3.2.1.2. Advanced control methods. Conventional FOWT controllers can easily realize SISO controllers; however, they may not be a suitable option for highly coupled multi-objective systems such as FOWTs. The design process of SISO controllers requires a thorough understanding of the system and careful tuning of the control loops. Otherwise, multiple control loops may couple with each other and affect the overall system performance. As suggested by Jonkman et al. [20], advanced controllers based on MIMO may further improve the performance of

FOWTs, owing to their inherent ability to deal with short SISO control. MIMO control schemes such as LQR, LPV, and MPC, used for FOWTs reported in the literature are discussed in the following.

Most of the advanced controllers designed for FOWTs are based on state-space control, where the design involves linearizing the nonlinear system model at an operating point x_{op} such that state x transforms into the deviation Δx around x_{op}. Later, the linear control theory was applied to design a controller to achieve the given objectives. The state-space equations are as follows:

$$\begin{aligned}\Delta\dot{x} &= A\Delta x + B\Delta u + B_d\Delta u_d\\ \Delta y &= C\Delta x + D\Delta u + D_d\Delta u_d\end{aligned} \tag{3}$$

where

- $x = x_{op} + \Delta x$
- y= Measurement matrix
- Δu= Actuator matrix
- Δu_d= Disturbance matrix
- A = State matrix
- B = Actuator gain matrix
- B_d= Disturbance gain matrix
- C= Output matrix
- D= Feed-through inputs
- D_d= Feed-through disturbance

Several advanced controllers have been designed to deal with platform motions using the MIMO (LQR) methodology on barge, TLP, and spar-buoy platform-based FOWTs operating in region III [23–25]. The LQR collective blade pitch controller (LQR-CBPC) and individual blade pitch controller (LQR-IBPC) were designed for a barge platform [23]. The LQR-IBPC and wind disturbance-based disturbance-accommodating control (LQR-IBPC-DAC) were designed for FOWTs on a barge and TLP [25]. The controllers designed for the barge and TLP were later used to investigate the performance of a spar-buoy platform [24].

In region III, the LQR-CBPC scheme for FOWT showed improvements in speed regulation, mainly because of the use of constant-power control instead of constant-torque control and platform pitch motion reduction. However, using the CBP mechanism led to increased tower loads due to overlapping blade pitch commands issued for rotor speed control and platform pitch minimization [24]. To circumvent this issue, LQR-IBPC was used, as in the IBPC mechanism, asymmetric rotor loads are created by pitching blades separately, in contrast to the CBP mechanism, and the overlapping blade pitch commands for rotor speed regulation and platform motion suppression are resolved. The LQR-IBPC mechanism improved the tower loading for the barge platform. In comparison, the performance of LQR-IBPC was found to be limited because of the relatively lower platform frequency of the spar-buoy platform. However, LQR-IBPC has the advantage of improved rotor and power regulation based on increased blade pitch actuation for the spar-buoy platform.

The LQR controller based on IBPC achieved improvements when applied to the barge platform compared to the LQR-CBPC control [23]. LQR-IBPC-DAC was not determined to be unsuitable for barge platforms, because the barge platform is mainly influenced by waves, whereas the LQR-IBPC-DAC is used to address wind disturbances. [25]. LQR-IBPC was shown to improve the rotor speed and power regulation for barges and TLPs, but in terms of dealing with platform pitching, this scheme was not as effective for spar-buoys because of the low natural frequency of the platform. Furthermore, improvements related to power and speed regulation were achieved using the LQR-IBPC-DAC for the TLP.

A collective blade-pitched H-infinity control (H-Infinity-CBP) based on a simplified semi-submersible FOWT nonlinear model [57] was used to deal with the platform motion and associated power regulation and load mitigation by Sanchez et al. [58]. H-Infinity-CBP is designed based on a linearizing nonlinear model operating in region III. Rotor speed regulation of up to 40% was achieved, including relatively smaller improvements in platform pitch motion reduction and load mitigation.

A study was conducted on the input–output relation of a 10 MW FOWT to determine the frequencies with a substantial impact on the output with the least control variable impact by Lemmer et al. [59]. The wave information was added to construct a realistic environment and to represent the coupled frequencies using the parametric wave excitation model [60]. Wind and wave disturbances with a significant impact on the output due to the minimum control actuation were chosen. This information was used to design an LQR controller based on the input blade pitch angle and generator torque, and it was compared with a conventional PI controller. The designed controller was observed to have improvements in system response reduction and damping various resonances. However, the control mechanism could not completely overcome the effect of the incoming wave disturbance.

Gain-scheduled (GS) output feedback H-infinity control based on the collective blade-pitch approach for FOWTs operating in region III was designed by Bakka et al. [61]. A simplified model is generated based on significant FAST [55] model dynamics for control synthesis, namely, the rotor generator and tower. Linear models were generated at multiple operating points based on output feedback H-infinity control, and a scheduling mechanism was developed. Substantial improvements were found in terms of tower loading and rotor speed regulation.

Input/output feedback linearization (IOFL) and sliding mode control (SMC) methods were used to analyze the effects of incident disturbance on platform motions and regulate the generator speed and of FOWTs operating in region III [62]. A simplified model based on the DOFs of the blade pitch, generator speed, and platform pitch was obtained. Later, a simplified nonlinear model based on a series of linearized simplified models was designed. The switching mechanism between these linear models was obtained based on the LPV model as a blade pitch angle function. Compared with the baseline model, SMC showed improvements in generator speed regulation, while the platform pitch motions were similar to those of the baseline wind turbine. The reason for speed regulation was that the wind speed was considered for the control design. However, platform motions were observed without revising the control design. In contrast to SMC, IOFL control causes increased platform pitching motion in comparison to the baseline controller [20]. Another important finding was that the performance of the developed controller was degraded when implemented in complex models.

LPV and LQR were developed by using a GS blade pitch controller for a barge platform-based FOWT [26]. The objective was to regulate the generated power and minimize the structural loading while operating in region III. The LPV was further modified with state feedback and output feedback control mechanisms and compared with the baseline wind turbine [20]. It was found that the GS-LPV and GS-LQR controllers performed better in terms of power regulation and platform pitch minimization. In contrast, the LPV-GS controller with state feedback showed superior improvements in platform pitch motion damping compared to the other controllers.

A collective blade pitch switching LPV (CBP-SLPV) was proposed based on a semi-submersible FOWT to deal with the platform motions and associated power regulation over the entire region III [63]. The SLPV was developed based on a simplified nonlinear model [57] by linearizing over a range of operating points in region III. Satisfactory generator speed and power regulation were achieved in comparison to the baseline controller [20].

MPC is an advanced control method that predicts future action based on the available information of the internal system model, fulfilling a set of constraints. Numerous examples are available in the literature regarding the use of MPCs for fixed-bottom wind turbines. [64–67]. Schlipf et al. [27] designed a CBP-based nonlinear MPC (NMPC-CBP) for FOWTs operating in region III based on the simplified Sandner model [68]. Incident wind and wave previews were used for the controller design based on the blade pitch and generated torque. The control objective was to keep the generated power and rotor speed steady based on an ideal estimation of the wind and wave previews [64]. The designed controller was later compared with the baseline FOWT [20] placed on a spar-buoy platform under intense wave and wind profiles. The controller showed satisfactory results regarding the generated power and speed regulation error, including the blade load reduction; however, the NMPC controller requires higher computational resources.

Following the CBP-based nonlinear MPC-CBP design for FOWTs in [27], Raach et al. [28] developed an extended version of NMPC based on the IBP mechanism (NMPC-IBP). NMPC-IBP includes rotor and blade load reductions alongside the existing benefits of the original NMPC-CBP, platform pitch reduction and rotor speed regulation. After the controller design, it was successfully implemented on the baseline wind turbine exposed to turbulent loads. Rotor fatigue loads were reduced significantly by using the extended NMPC based on the IBP mechanism.

An optimal linear MPC was implemented on a 10 MW FOWT by Lemmer et al. [29]. A tunable controller was designed to provide early-stage design assistance during FOWT fabrication. The linear MPC based on the MIMO system was designed to operate in region III to regulate the power to a constant value and minimize the structural loads. In comparison, maximum power generation was the primary objective for region II. The linear MPC showed superior improvement to a PI controller for rotor speed and generator power regulation. Moreover, tower-top movement and negative platform pitch were minimized.

A reduction in the LCOE of an FOWT may be achieved through enhanced structural performance against incident loads. For this purpose, we discuss several feedback controllers. One major drawback is that these control mechanisms are designed to respond to incidents after their interactions with the system structure. The wind turbine structure of an FOWT experiences the incoming wind, and the wave and feedback control system is activated after the interaction of incoming wind and waves with the system. Such interactions may degrade structural life over a period of time. Thus, conventional controllers may not achieve extended structural life and would subsequently increase the LCOE.

To circumvent the shortcomings of feedback controllers, researchers may use feedforward control loops to deal with incident disturbances before contacting the wind turbine. LIDAR has been used to measure incoming wind disturbance. Numerous attempts have been made to use LIDAR for bottom-fixed wind turbines [69–71]. LIDAR is based on Doppler's principle, where a laser beam is spread out and received upon reflection [72]. The wavelengths of the transmitted and received beams are used to estimate the incoming wind speed. Two types of LIDARs are available based on wind speed calculation methods, that is, continuous and pulsed waves. Continuous-wave LIDAR uses a laser beam focused at the focal point, whereas pulsed-wave LIDAR calculates the wind speed at multiple distances [69].

Unlike bottom-fixed wind turbines, preview-based LIDAR-assisted control for FOWT is still under development. An extended version of feedforward CBPC, initially used for bottom-fixed wind turbines in [73], was designed for FOWTs using H-infinity control synthesis by Navalkar et al. [30]. Based on the combination with feedforward feedback, the newly formulated CBPC was found to be useful for minimizing the loads and generator speed oscillations. Schlipf et al. [31] designed a CBP-feedforward controller (FF-CB) for FOWTs based on LIDAR data. The feedforward control was designed using a simplified nonlinear model for ideal wind preview and used along with the conventional feedback controller designed by Jonkman et al. [55]. Later, the design procedure was followed by using nacelle-based LIDAR information instead of an ideal preview wind. With the addition of wind uncertainty, a realistic feedforward controller proved useful compared with the standalone baseline controller to minimize rotor speed and power fluctuation and reduce blade, rotor shaft, and tower loads.

3.2.2. Mass–spring–damper based FOWT control methods

An alternative approach was reported in the literature to minimize structural loads and external influences by introducing additional actuators based on a mass–spring–damper, known as structural control (SC). In this methodology, additional DOFs are introduced to influence the structural behavior of the system. This methodology has been widely used to minimize the oscillations and vibrations of mechanical structures and systems efficiently [74–77]. For FOWTs, the aim of using the SC is to dampen platform oscillations and tower loading. The critical advantage of the SC for FOWTs was observed while operating in region III. The blade pitch mechanism is not required to regulate platform stability, a significant issue observed in region III, and SC addresses the platform's pitching phenomenon. The SC is based on passive, semi-active, and active control approaches [78]. Passive structural control systems use a set of constant parameters to dampen the oscillations. Semi-active controllers are mainly tunable over a period of time. Contrary to the passive control approach, active structural control differs based on generating restoring forces with dedicated actuators to address the structural loading and oscillation.

Passive and active structural control schemes based on two independent tuned mass dampers (TMDs) to deal with the loading and damping of platform oscillations were designed by Lackner et al. [36]. These TMDs were placed in the nacelle of a floating barge operating in regions II and III. Lackner et al. [36] modified the baseline wind turbine [20] by integrating TMD systems and incorporating passive, semi-active, and active structural control synthesis. Based on the input–output data, a high-order design model was created using system identification. Control synthesis was achieved based on the loop-shaping mechanism. It was observed that both techniques reduced wind turbine loading when compared with the baseline wind turbine. However, the complexity and overall cost increased owing to the addition of TMDs. Moreover, active structural control outperformed in reducing the tower's fore–aft fatigue load at the expense of energy consumption, which may be obtained from the high wind while operating in region III. However, in region II, active structural control proved costly, and for this purpose, a hybrid mass damper (HMD) was incorporated to act as a passive TMD while operating in region II.

Nacelle-based TMD systems used by Lackner et al. [36] were redesigned by Namik et al. [79] to examine the impact of actuator dynamics on TMDs. Load reduction and power consumption were also investigated for passive and active control strategies on a barge platform-based FOWT. Although the newly designed controllers followed the simulation trends as reported by Lackner et al. [36] concerning load reduction, the redesigned TMD system achieved platform pitch minimization by consuming less power on average.

Simplified models of the mono-pile, barge, Hywind spar-buoy, and TLP were used to design an optimal passive TMD based on the genetic algorithm proposed by Stewart et al. [80]. This TMD was found to reduce the side-to-side tower fatigue load, which is one of the main components of the fatigue loads of FOWTs, better for barge and mono-pile than the TLP and spar-buoy platforms.

A semi-active TMD placed in the nacelle of a wind turbine was used to minimize the incident loads for two platforms: bottom-fixed and TLP, while operating in regions II and III [81]. The designed semi-active TMD has a low-power energy source, and it swiftly switches between the active and passive modes. This mechanism minimizes the side-to-side tower loading of the monopile and slackline incidents for the TLP. A platform-based TMD for barge platform FOWT was used to minimize the platform motions and tower loading while operating in regions II and III [82]. A simple static output-feedback mechanism was proposed to generate stroke using generalized H-infinity control. An input–output linear model was obtained using system identification. Improved results were obtained in terms of fatigue load and generator power error reduction, whereas upon comparison, the generalized H-infinity control achieves superior performance to H-infinity structural control. Similarly, a multilayered tuned liquid damper (TLD) was developed in [83] for a spar-buoy floating platform, and it was found to be useful for minimizing platform motions.

The performance of the conventional passive TMD system was improved by introducing an inerter in the system [84]. The proposed TMD system was placed in the nacelle of the FOWT attached to a barge. The improvement was evaluated under the influence of real incident disturbances, waves and wind. This novel extension of the TMD was found to be helpful in reducing tower loading. In a relatively similar approach, a sewing thread artificial muscle (STAM) based on thermal actuation attached to the mooring lines of the TLP was proposed to minimize platform pitching and tower loading for regions II and III [85]. The active mooring method showed improved results for the tower loading and pitching motions.

4. Wind and wave forecast algorithms for FOWT control

Incident disturbance forecasting is an essential feature of advanced control algorithms, such as MPC and feedforward control. Unlike feedback control, where the controller responds to the disturbance after the system interacts with it, feedforward controllers react to the preview of the incoming disturbance ahead of its contact with the system. This approach improves the performance because the incident disturbance preview provides the controller with sufficient time to respond to the incoming disturbance and adjust parameters to achieve control objectives. Preview-enabled control also enhances the system's structural life as it responds to the incident disturbances ahead of its contact with the system structure.

FOWTs are exposed to incident wind and wave disturbances that propagate in the ocean. Many controllers are designed to stabilize the platform and achieve control objectives by minimizing the effects of wind and wave disturbances. However, the performance and structural life of FOWTs still lags behind those of fixed bottom offshore wind turbines, as most of these control systems are based on feedback control. The incident wind and wave prediction may effectively improve the performance, loading, and structural life of FOWTs with the help of advanced control algorithms such as MPC or feedforward control, as demonstrated by LIDAR-based incident wind preview-enabled feedforward controllers [31].

Several forecast techniques for wind and waves have been reported in the literature, which can be used for preview-based advanced controllers. However, there are issues concerning the prediction horizon length, and the forecast quality should be considered when using these prediction mechanisms. In this section, wind and wave forecasting algorithms are discussed.

4.1. Wind forecasting

The wind turbine industry extensively employs wind forecasting to examine a region's seasonal power production, grid integration, and wind farm design [86]. Based on its application, the length of the prediction horizon of wind forecasting ranges from a few hours to months and is categorized as short-, medium-, and long-term. However, the prediction horizon length for individual wind turbine control systems based on preview information is only a few seconds. Advanced controllers such as feedforward control require a preview time of a few seconds [48]. Similarly, MPC uses a 5–10 s horizon to compute the input values for the system response [49]. Therefore, the scope of this review is limited to wind forecasting for wind turbine control, referred to herein as ultrashort wind forecasting. An overview of the models and devices used for ultrashort wind forecasts is provided as follows.

Statistical time-series models used for wind forecasts are based on historical site data. Based on historical wind data, these models tend to learn the underlying patterns in the available data and calculate future values ahead of time. Widely used conventional statistical models for wind forecasting include the autoregressive model (AR) [43,87], autoregressive moving average model (ARMA) [44], autoregressive integral moving average (ARIMA) [45], fractional-ARIMA [46], and Hammerstein autoregressive (HAR) [47]. Statistical methods rely heavily on historical wind data, and thus may provide faulty wind forecasts in the absence of sufficient historical site data.

Machine learning (ML) techniques rely on historical data and consider the atmospheric variables that affect wind speed, such as humidity, elevation, and atmospheric pressure, for wind forecasting. Therefore, ML methods deal with the nonlinearity of wind better than statistical methods. ML nonlinear prediction methods include artificial neural networks (ANNs) [88,89], recurrent neural networks (RNNs) [90], support vector machine (SVM) [91,92], least-squares support vector machine (LSSVM) [93,94], Gaussian process (GP) [95], Bayesian networks [96], and extreme learning machine (ELM) [97]. Overfitting and minimum local existence are major drawbacks of ANNs [98]. ELM has been proven to have better performance than conventional ANNs and is used for both speed estimation and power forecasting [97,99,100]. Hybrid models, combinations of existing model techniques, have also been reported in the literature for improved performance. For example, a linear ARIMA and a nonlinear ANN were used in combination to improve wind forecasting [101]. Similarly, a combination of ELM and ARIMA was shown to have enhanced performance for wind forecasting [102].

LIDAR is used in the wind turbine industry for several applications, such as wind power estimation and site analysis [103]. It is also used to provide the preview of incident wind for an ultrashort scale horizon upstream of the wind turbine. The wind speed is calculated based on laser light emitted from the LIDAR and reflected by incoming wind particles. Preview-based measurement of the incoming wind speed for FOWT control is discussed in Section 3. LIDAR-based forecasting techniques have been reported to outperform forecasting techniques such as ARIMA and persistent methods [104,105]. However, the higher cost and weather-dependent performance are challenges that require further research.

4.2. Wave forecasting

Incident waves account for a significant part of the FOWT loads when minimizing platform motions. Therefore, they are an essential feature to be considered alongside the incident wind in preview-based FOWT control. Feedforward controllers based on wind and wave previews may improve the FOWT loading and platform stability compared to feedback controllers by providing the system with sufficient time to deal with the incoming disturbances. Many wave forecast methods have been reported in the literature, such as physics-based models, statistical models, and ML models. A discussion of these models is provided in the following.

Physics-based models are numerically designed models that solve the complexity of waves based on the physics behind wave mechanics. Physics-based wave forecast models include WAVEWATCH III (WW3) [106], European Center for Medium-range Weather Forecasts (ECMWF) [107], and Simulating Waves Nearshore (SWAN) [108]. These models are generally used for long-term prediction horizons over extensive areas. In contrast to physics-based theory-driven models, data-driven statistical and ML provide accurate predictions based on historical site data. These time-series algorithms extrapolate past values to provide future wave predictions. Statistical wave prediction models for wave prediction reported in the literature include AR, ARMA, and ARIMA [109–111]. Compared to statistical models, ML prediction models provide improved nonlinear trend identification in time series wave data. ANN, RNN, CNN, and ANFIS-based prediction models [112–116] are examples of ML models used for wave prediction in the literature. A comparison of time series-based models and a physics-based model (ECMWF) at multiple sites highlights the weaknesses and strengths of these models [117]. The physics-based model performs better for longer prediction horizons, whereas the time-series models are better for a shorter prediction horizons. Combinations of physics-based and data-driven statistical models have also been reported in the literature [118,119].

Table 2
Conventional FOWT control methods based on blade-pitch mechanism.

Method	Model	Platform	Description	Economic viability	OR
CBP-GSPI [19]	HAWC2/SIMO-RIFLEX	Spar-buoy (Hywind)	Region-dependent control based on simple switching process, pitching controller of frequency lower than the platform pitching frequency is employed for region III.	Improved tower stability. however, degraded power quality and poor rotor speed regulation.	2,3
CBP-GSPI [20,56]	FAST	Barge, TLP, Spar - buoy	Feedback loop based on Tower-top movement, pitch-to-stall regulation and detuned gains.	Only detuned gains control improves the negative damping issue. Further use of MIMO control is suggested including IBPC.	2,3
Simple Platform Pitch Control [21]	FAST	Barge	Platform pitch velocity based generator speed control in region III. Also used IBPC.	Reduced negative damping and blade pitch activity at the cost of the rotor speed fluctuations and power variation. IBPC showed inadequate load reduction.	3
Control based on estimated wind speed [22]	HAWC2/SIMO-RIFLEX	Spar-buoy (Hywind)	Estimator based control mechanism.	Tower Loading, nacelle oscillation and rotor loads are found reduced. However, poor rotor speed regulation and reduced power generated are observed.	3

4.3. Consideration of wind and wave prediction

Wind and wave preview-enabled advanced controllers can be a great solution for lowering the cost of energy. Look-ahead incident disturbance information is crucial, as LIDAR-assisted wind preview-enabled controllers are useful for FOWTs [31]. Ultrashort incident wind and wave forecast methods have the potential to improve the performance of advanced controllers [120]. However, associated issues need to be addressed before their application in FOWT control algorithms.

- Statistical and ML models generally perform better for a shorter horizon, as these models are solely based on historical data. ML models such as ANN and RNN perform better than statistical models, because they have the ability to map nonlinear trends in a given dataset [37]. However, because these prediction methods are based on the historical data, specific problems are apparent, such as a lack of sufficient site data, poor anomaly detection, and scalability.
- Physics-based weather models such as [106–108] are often suitable for predicting longer horizons. A combination of physics-based models with short-term ML forecast models can be a viable avenue for wind turbine control. The shortcomings of ML techniques can be mitigated using extensive data generated through physics-based models.
- LIDAR-assisted wind prediction is a superior alternative, as the prediction range is up to 30 km [72]. However, because the working principle depends on the line of sight, performance can be affected by poor weather conditions.

5. Discussion

FOWT technology is still in the precommercial phase, in contrast to bottom-fixed offshore wind turbines. The primary concern of FOWT development is the associated cost of energy production and the potential to achieve a cost-effective advantage compared to the bottom-fixed systems, which is deteriorated by the floating base of FOWTs. However, an efficient control mechanism may deal with the shortcomings of the platform, making it economically feasible. These control methods aim to lower the LCOE while operating the regions below and above the rated wind speed, making it economically feasible. Several control schemes have recently been developed for this purpose.

5.1. Comparison between blade-pitch and mass–spring–damper based FOWT control methods

FOWT can be controlled based on either existing actuators, known as blade-pitch controller methods, reported in Section 3.2.1 or by including additional actuators, mass–spring–damper-based FOWT control methods Section 3.2.2. We compare these control methodologies in detail.

When considering blade-pitch controller methods, conventional SISO feedback controllers are a natural choice for FOWTs by manipulating the aerodynamic wind load using the blade pitch angle and generator torque. Their simple design and easy realization make them suitable options for bottom-fixed wind turbines. However, the natural frequency of the floating platform is lower than that of the bottom-fixed wind turbine foundation, which causes negative platform damping in region III [19]. Therefore, controllers designed for bottom-fixed wind turbines may increase negative platform damping when used for FOWTs. Several SISO control strategies have been reported in the literature to address this issue; refer to Table 2 for details. For example, negative platform damping is addressed by reducing the control bandwidth; however, power and speed variations have been observed [19]. Skaare et al. [22] developed a wind speed estimator-based blade pitch control method to deal with the floating motion of the platform. Improvements in platform motion damping were achieved at the cost of the rotor speed and power output deviation. Jonkman et al. [20] utilized a GS SISO controller with detuned gains to deal with negative platform damping on a barge platform. However, the achieved performance is likely to be increased using MIMO controllers, as suggested by Jonkman et al. [20]. The coupling between the unmodeled DOF and SISO control loops of the FOWT causes inadequate platform motion minimization, as well as power and rotor speed regulation.

Blade-pitch-based advanced control methods can deal with cross-coupling between the unmodeled system dynamics and control loops better than SISO controllers. These controllers are based on linearized system models and exhibit superior performance compared with the baseline SISO controller. The conflicting blade-pitch commands for the platform and rotor regulation are dealt with by the IBPC by creating an asymmetric rotor load. However, the platform properties may affect the performance of these advanced controllers. For example, the barge platform is prone to increased loads owing to the inherent platform motion that induces incident waves. In the case of a TLP, the platform is less affected by the incident waves. Thus, the performance of control methods differs [25].

Most of the blade pitch advanced control methods for FOWTs are designed around a single operating point. The control method may perform well around the operating point; however, moving away from the operating point may lead to performance degradation. To overcome this obstacle, a GS controller based on a series of linearized models at a range of operating points improves power regulation and platform motions. LPV controllers offer another switching mechanism to incorporate multiple linear models for a range of operations and deal with the limitations of linearized MIMO models that are only valid around linearization points.

Advanced controllers, such as MPC controllers, improve performance while dealing with uncertainties and unmodeled system dynamics. Based on preview wind and wave measurements, MPC corrects the control trajectory based on the plant model at every step. It also allows

Table 3
Advanced FOWT control methods based on blade-pitch mechanism.

Control methods	Model	Platform	Description	Economic viability	OR
LQR-CBP [23]	FAST	Barge	CBP based Rotor thrust is used to regulate platform pitch and rotor speed.	Poor power and rotor regulation compared with baseline controller. Improved tower loading, platform motions.	3
LQR-IBPC [23–25]	FAST	Barge, TLP, Spar-Buoy	Asymmetric rotor aerodynamic load is used to regulate the platform pitch and rotor speed.	Tower loads are decreased for the barge, however poor rotor and power regulation. TLP, compared to the Barge and spar-buoy, exhibits less platform movement when IBPC. Due to the lower natural platform frequency, IBPC on Spar-buoy is not useful regardless of the improved rotor regulation.	3
LQR-IBPC-DAC [24,25]	FAST	Barge, TLP, Spar-Buoy	DAC is used as an extension of IBPC with an additional wind disturbance rejection.	DAC has no further improvement on the barge compared to the IBPC applied on a barge. Whereas, when it is utilized on TLP, power and speed regulation are improved with a reduction in side-to-side loads. DAC used on spar-buoy improves rotor speed but increases the blade pitch activity and loads.	3
H-Infinity-CBP [58]	Hommer model	Semi-submersible	Linearized MIMO control method	Improved rotor speed regulation and load reduction compared to baseline wind turbine.	3
MIMO (LQR) [59]	DTU-10MW	Spar-Buoy Triple Spar	Effects of the control inputs are analyzed based on how they affects the output for a floating wind turbine in an open loop scenario and an LQR based on observations is synthesized.	Damped various resonances, but observed not being able to suppress the wave excitation entirely.	3
GS-Output feedback H-infinity [61]	FAST	Barge	Generator speed is regulated at the rated value using a gain scheduled controller to keep drive train and tower oscillations low.	Improvements in platform stability and reduced fatigue loads, LPV based GS controller is suggested for further improvements.	3
SMC and IOFL [62]	FAST	Barge	Methods based on LPV control are implemented; to regulate generator speed, and to analyze the effects of incident disturbance on platform motions.	SMC is found to have achieved generator speed regulation better than IOFL for simplified wind turbine models and performance degraded when complex wind turbine models are utilized.	3
LPV and LQR based GS [26]	FAST	Barge	GS-LPV and GS-LQR based on output feedback and state feedback are employed.	Improved power regulation and platform pitch minimization is achieved.	3
SLPV [63]	Hommer model	Semi-Submersible	Switching lpv based on simplified model is utilized.	Improvements in generator speed and power regulations are key enhancement .	3
NMPC (CBP) [27]	Sandner Model	Spar-buoy	NMPC based on CBP mechanism and generator torque is employed.	Enhanced performance in terms of rotor regulation, platform motion minimization and improved loads. However, the computational cost is significantly higher.	3
N-MPC (IBP) [28]	Sandner Model	Spar-buoy	IBP mechanism is extended based on the collective blade pitch approach.	Lowered pitch and yaw motion, improved speed regulation and reduction of the loads on blades.	3
Linear - MPC (CBP) [29]	Sandner Model	Modified Spar	Linear-MPC based MIMO system is deigned using CBC approach.	Speed and generated power regulation. Improved negative platform pitch motions.	2,3
LIDAR (FF-CBPC) [30]	FAST	TLP	Feedforward controller based on CBP mechanism is introduced for wind speed regulation.	Improved speed regulation and minimized the loads.	3
LIDAR (FF-CBPC) [31]	FAST	Spar-buoy	CBP FF controller is formulated based on ideal wind speed estimation.	Improved rotor speed and power regulation, along with blades, rotor, and tower load reductions.	3

designers to include the constraints on inputs and states in the control design, thus effectively avoiding physical saturation. However, MPC is a computationally demanding control mechanism for complex systems, such as FOWTs. Advanced controllers based on preview information on incident disturbances are superior alternatives to feedback controllers. LIDAR is a valuable addition for improving bottom-fixed wind turbines; however, LIDAR performance is yet to be evaluated for FOWTs exposed to wave disturbances. Details of advanced MIMO controllers are provided in Table 3.

Mass–spring–damper-based FOWT control methods adequately reduce pitching phenomena and wind turbine loads. These control methods include additional DOFs to deal with platform motions and tower load, unlike blade-pitch control methods. In this way, the controller mechanisms ease the high blade pitch activity and provide further performance improvement. However, the addition of extra DOFs causes an increase in the complexity of FOWTs. Moreover, the power required to generate a heavy stroke in active dampers requires further investigation regarding cost-effectiveness on an industrial scale. A list of existing mass–spring–damper-based FOWT controls is provided in Table 4.

5.2. Comparison of control algorithms on different platforms

As described earlier, the development of control strategies is usually co-designed with a specific FOWT system; thus, it is still unknown which control algorithm has the potential to be the most cost-effective across generic platforms. Nevertheless, it is worthwhile to develop an evaluation matrix for load mitigation, power regulation, and platform motion minimization for each type of generic platform to provide guidance to technology developers and relevant researchers. Table 5 assesses the benefit of certain advanced MIMO controls to the four types of platforms by scoring the associated improvement from 1 (decrease in performance) to 5 (massive improvement). Because the mass–spring–damper-based control is still in the conceptual stage, only blade-pitch-based control algorithms are considered.

As shown in Table 5, the LQR controller can suppress platform motion to a certain extent over all four types of platforms, whereas it has a negative impact on the power regulation of the barge type. This is because the barge platform has a large moment of inertia in rotational modes, and thus the low-frequency blade-pitch control action is likely to lead the platform to achieve its resonance, resulting in a compromise

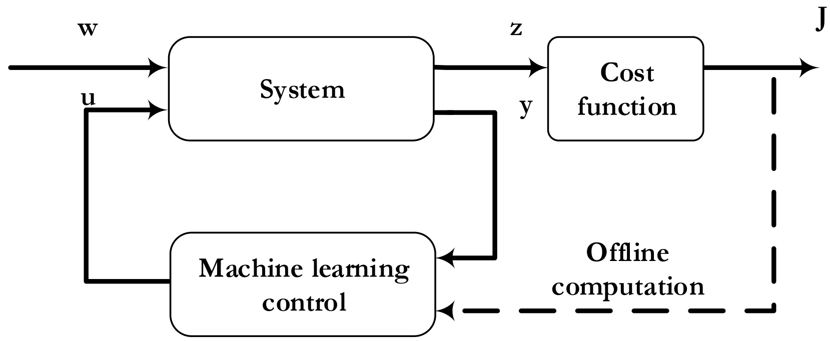

Fig. 8. Machine learning control.

in the power regulation. Because feedforward controllers and nonlinear model predictive controllers utilize predictions to manipulate the system's dynamics, they can result in a significant improvement in power regulation and platform motion suppression. However, as nonlinear model prediction usually leads to a heavy computational burden, the corresponding cost could significantly increase. H-Infinity controllers have almost identical performance to LQR controllers over the given platforms, because their conservative nature tends to choose suboptimal control actions. Regarding SLPV controllers, owing to a lack of information, their excellent performance in power regulation and platform motion suppression can only be confirmed for semi-submersible platforms.

Overall, one can say that the nonlinear model predictive controller is the most preferable for generic platforms. The main concern of computational loading can be addressed by using high-performance cluster computing or a learning-inspired method in the near future.

5.3. Outlook and potential improvements

The majority of control mechanisms were developed using model-based design. In complex systems such as FOWTs, accurate system modeling is essential for dealing with model uncertainties and complex incident disturbances, such as wind and waves. In an ideal situation, the plant represents the actual systems and actuators, whereas in reality, it is only a fair approximation of the system. Model-based FOWT models are generally a reasonable choice for designing controllers, as shown in Section 3.2; however, they may require considerable effort for controller synthesis and tuning. Model-based system models are usually designed based on approximations, which may result from a poor understanding of the system and unmodeled dynamics, leading to a compromise in system performance. In this case, the model-free control approach may be utilized to represent the plant model and deal with the aforementioned shortcomings not addressed by first-principles mathematical modeling. Input–output data may be used to deduce a plant representation for the respective controller design after careful assessment and performance evolution. Unlike model-based design, data-driven model-free controllers do not rely on the system characteristics, eliminating the need for controller dependency on the plant model. Furthermore, unlike the model-based control approach, in model-free methodologies, system stability does not rely on model accuracy [121]. ML techniques may address this issue by finding the optimal control laws by mapping the output of the sensors to control the actuators. These techniques are based on bio-inspired computational methods, including genetic algorithms, reinforcement, and iterative learning [122]. These algorithms may be used to minimize constraint-based cost functions designed according to the control objectives. One such example of machine learning control (MLC) usage for complex structures such as FOWTs has been reported in the literature [123]. The input–output data are correlated to form a control law $u = k(y)$ and evaluated using a cost function J, as shown in the schematic in Fig. 8. It shows improved performance compared to the baseline controller and demonstrates a viable solution for further research on the complex control synthesis of FOWTs.

The complex nature of the incident wind and wave limits the control design for FOWTs. Instantaneous changes in these disturbances, such as wind and wave gusts, may affect the design of control methods for FOWTs. Moreover, if not considered, the stochastic nature of these flows may also degrade the structural life and performance of wind turbines. Incoming disturbances may be modeled to circumvent these issues. However, it is challenging to design perfect mathematical models of incident wind and waves, owing to their inherently complex properties and high dimensionality. Data-driven ML plays a promising role in solving complex real-life problems. Dynamic mode decomposition [124], sparse identification of nonlinear dynamics [125], and Koopman operator theory [126] are data-driven methods that may be used to understand complex turbulent flows and interpret the underlying behaviors. Simplified models of the incident wind and wave disturbances may improve the incoming disturbance prediction and estimation process based on these techniques. The LCOE of large FOWTs can be reduced by better understanding the effect of incident disturbances on FOWTs and subsequently implementing efficient control design.

6. Summary

In this article, we have thoroughly presented a range of control algorithms for FOWT system dynamics, including blade-pitch type and mass–spring–damper type. Blade-pitch-based control methods utilize existing FOWT actuators to achieve platform-associated motion suppression, power regulation, and load mitigation. Mass-spring control methods are based on the addition of extra actuators to deal with platform motions, power generation, and load minimization issues. Although, these control methods decouple the use of blade-pitch actuators that compete for platform motion suppression and rotor regulation, the increased system cost and complexity are the main obstacles for their practical application. Furthermore, it was found that the integration of model prediction into blade pitch-based control usually leads to a significant improvement in power regulation and load mitigation over all types of platforms, highlighting the importance of wind and wave forecasting. Finally, model-free control and learning-inspired control may be potentially viable solutions to the complex operational scenario of the FOWT in the future.

Based on the understanding of the existing methods discussed earlier, we tentatively make some recommendations for future analysis:

- Experimental validation of the blade-pitch control methods with complex wind and wave environment is suggested. Further, it is recommended to benchmark the performance of these control methods across different floating platforms.
- Mass–spring–damper-based FOWT control methods may be further investigated as a viable solution for pitching phenomena and wind turbine loading. Their ability to minimize platform pitching

Table 4
Advanced FOWT control methods based on Mass–spring–damper mechanism.

Control methods	Model	Platform	Description	Economic viability	OR
Active and passive TMD [36]	FAST-SC	Barge/ Bottom-fixed monopole	TMD placed in the nacelle, H-infinity based loop shaping controllers.	Reduced tower loading, Increased complexity and power consumption due to active-TMDs.	2,3
Improved Active and passive TMD [79]	FAST-SC	Barge	Nacelle based redesigned TMDs taking actuator model into consideration.	Fore–aft loads reduction and tower base bending minimization.	2,3
Optimal Passive TMD [80]	FAST-SC	Mono-pile, barge , Hywind spar-buoy and TLP	Optimal passive TMD is developed based on available platforms using genetic algorithm.	Fatigue loads are found reduced for barge and mono-pile better than the TLP and Spar buoy.	2,3
Semi active TMD [81]	FAST-Orcaflex	Mono-pile and TLP (Pelastar)	Nacelle based semi-active TMD.	Minimized side-to-side tower loading of mono-pile and slackline incidents of TLP.	2,3
Active TMD [82]	FAST-SC	Barge	Platform-based TMD, A static output-feedback mechanism is proposed using a generalized H-infinity control	Fatigue load and generator power error is reduced while reliability and robustness issues of controller designed are found.	2,3
TLD [83]	Numerical methods	Spar-buoy	Nacelle based single and multilayer TLDs are examined and validated.	Enhanced platform pitching motion based on Multilayer TLD than single layer TLD.	–
Passive TMD [84]	FAST-SC	Barge	TMD placed in nacelle, Inerter based damping mechanism.	Effectively reduced wind and wave induced loads in comparison with similar conventional TMD control.	2
Active Mooring line control based on STAM [85]	FAST	TLP	STAM-integrated mooring lines.	Platform motions (pitch and roll) and tower bending moment, are minimized.	2,3

Table 5
Performance comparison of advanced (MIMO) control schemes compared to baseline controller.

Control method	Platform type	Tower Loads	Power regulation	Platform motions	Cost
LQR-IBPC	Barge	3	1	3	2
LQR-IBPC-DAC		3	1	3	2
LQR-IBPC	TLP	2	3	3	3
LQR-IBPC-DAC		2	4	4	5
LQR-IBPC	Spar-buoy	2	3	3	3
LQR-IBPC-DAC		2	4	2	3
FF-CB		2	5	2	4
NMPC-CBP		2	5	3	5
NMPC-IBPC		2	5	3	5
H-Infinity-CBP	Semi-Submersible	2	3	3	3
SLPV-CBP		~	4	3	~

5=Massive improvement; 4=Major improvement; 3=Minor improvement;2=Slight improvement; 1=Decrease in performance.

phenomena without using blade pitch can provide designers with more freedom to design controllers. However, a cost-effective approach and subsequent validation studies are required.

- The effectiveness of preview devices such as LIDAR for FOWTs needs to be experimentally validated. Moreover, the inclusion of combined wind and wave prediction in the control design may elevate advanced control mechanisms, such as MPC.
- Further development is suggested regarding the use of prediction algorithms together with the use of physical devices such as LIDAR. Models based on ML tools would be of significant advantage in lowering the LCOE by understanding the underlying disturbance behaviors and designing optimal control laws.

Declaration of competing interest

The authors declare that they have no known competing financial interests or personal relationships that could have appeared to influence the work reported in this paper.

Acknowledgments

This work was supported by the National Key R&D Program of China (No. 2017YFE0132000 and No. 2019YFB1504402) and National Natural Science Foundation of China (No. 51761135012 and No. 11872248.The first author would like to thank Dr. Zeeshan Qaiser for discussion.)

Appendix A. Wind turbine

The working principle of the wind turbine deployed offshore is similar to the land-based wind turbines, which utilizes the blades to extract the kinetic energy from airflow and then convert the mechanical power into electrical power. The theoretical maximum efficiency of power harvested from wind is 59.3%, known as the Betz limit [127]. Maximum power (P_{max}) generated by a wind turbine in this scenario (see Fig. A.1) can be formulated as,

$$P_{\max} = \frac{1}{2}\rho A v^3 C_p(\lambda, \beta) \tag{A.1}$$

$$\lambda = \frac{\Omega R}{v} \tag{A.2}$$

where

- ρ= Air density
- A= Swept Area
- C_p = Power coefficient (based on tip-speed ratio (λ) and blade pitch angle β)
- R= Rotor radius
- Ω= Angular speed
- v= Wind speed

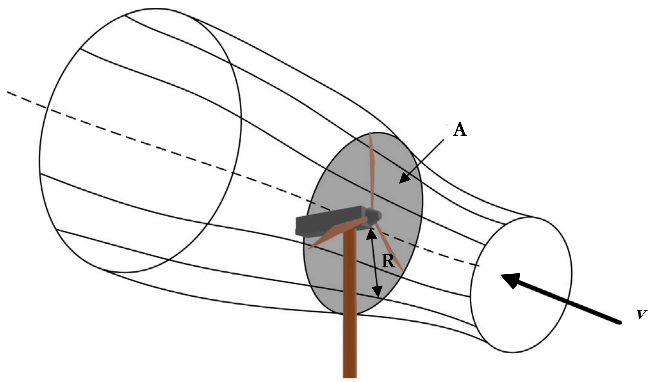

Fig. A.1. Wind energy extraction using wind turbine.

Appendix B. Simulation codes and models for FOWTs

The existing system models designed for the bottom-fixed wind turbines may not be able to reflect the dynamics of the FOWTs due to the complaint nature of FOWTs. Therefore, a system model is required to simulate the FOWTs that incorporates all the significant DOFs, including the floating base. A brief description of some of the major simulation codes used is given below.

Fatigue, Aerodynamics, Structures, and Turbulence (FAST)

The National Renewable Energy Lab (NREL) has designed a modular computer-aided engineering (CAE) open-source software Fatigue, aerodynamics, structures, and turbulence (FAST) to simulate wind turbines at a given operating condition [128]. FAST uses a multi-body/modal system (MBS) representation. The aerodynamics module is based on the blade element momentum (BEM) theory (quasi-static). At the same time, the hydrodyn modules offer modeling based on Potential flow and Morison's equation. Furthermore, models based on FAST can generate linearized models useful for the linear control design.

The widely-used standard multi-megawatt fictitious FOWT model, designed based on FAST is NREL 5MW baseline WT [55]. This utility-scale WT is developed based on the publicly available data of existing WTs and simulation models such as WindPACT [129], RECOFF [130], and DOWEC [131].

Horizontal Axis Wind Turbine Code-Second generation (HAWC2)

Horizontal Axis Wind Turbine Code-Second generation (HAWC2) is a time-domain commercial package that is mainly used to study the dynamics of fixed bottom WTs operating under externals loads [132]. The structural dynamics is based on MBS, and the aerodynamic module relies on BEM theory. The WT with a floating base is simulated using the SIMO/RIFLEX code coupled with HAWC2 [54], where SIMO/RIFLEX is used to model the floating foundation and mooring lines, whereas the rotor, blades, and nacelle are designed in HAWC2.

A next-generation 10 MW reference WT based on HAWC2 [133] similar to 5 MW baseline WT [55] is also available for the research and development.

Bladed

Bladed is a commercial software to simulate WTs for both onshore and offshore sites [134]. The FOWTs may be modeled using Bladed by considering the dynamics and the complexity of the system parameters. Bladed code also considers incident wave and wind loads, structural dynamics, aerodynamics, and suitable controller response.

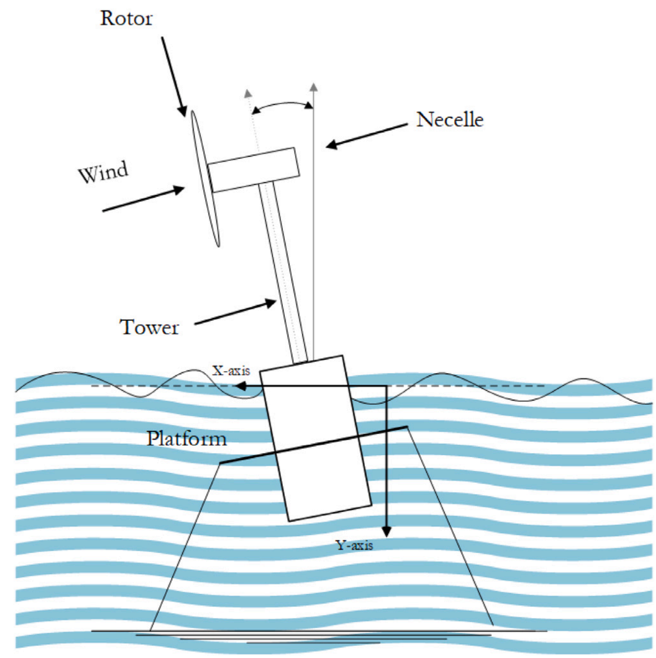

Fig. B.1. Adapted layout of Betti model [137].

The structural dynamics of the Bladed code are based on the multi-body modal system representation. The aerodynamic module uses both the momentum and blade element model. Simultaneously, an extended version of this model considers the effect of Prandtl's tip and root losses, dynamic wake models, and Glauert skew wake. The hydrodynamic module utilizes the penal method and Morison equation. With a built-in LIDAR module, Bladed code may be used to develop advanced control designs based on the LIDAR preview information. The Bladed code can generate the linearized model and state-space matrices, an essential part of linear control theory.

As a part of LEANWIND project [135] an 8 MW reference WT [136] is designed based on data available online of WTs and validated using Bladed.

SIMPACK

SIMPACK code is designed to simulate a range of industrial applications such as robotics, automotive aerospace, and railway systems [138]. It a general-purpose software based on MBS and is applicable for the WTs as well. An extension to the existing code is used for FOWT, connecting HydroDyn and SIMPACK with the help of SIMHydroDyn [139]. These additional modules are to deal with the hydrodynamics and the mooring lines of FOWTs.

A comparison of the parameters and properties of the 5 MW, 8 MW and 10 MW reference wind turbines is given in Table B.1.

Simplified models

Complex simulation codes like FAST are considered an appropriate choice to study the systems behavior, platform stability, and power quality under external disturbances. However, the complex nature of these models may cause problems in the control design process. To circumvent shortcomings associated with the complex models, a simple yet accurate model can be developed to model the essential dynamics and behavior of a FOWT with high accuracy. The effectiveness of simplified models for FOWTs in designing useful controllers has been proven [137]. To facilitate the simple control design process, researchers have produced simplified FOWT models. Below are a few noticeable models available in the literature.

Table B.1
Summary of 5, 8 and 10 MW reference wind turbines.

Turbine Name	NREL (5 MW)	LEANWIND (8 MW)	DTU (10 MW)
Number of blades and rotor orientation	3 blades, Upwind	3 blades, Upwind	3 blades, Upwind
Rotor Diameter (m)	126	164	178.3
Tower and Hub height (m)	90, 87.6	110, 106.3	119, 115.6
Cut in, cut out and rated wind speed (m/s)	3, 25, 11.4	4, 25, 12.5	4, 25, 11.4
Rotor speed range (rpm)	6.9, 12.1	6.3, 10.5	6, 9.6
Hub Nacelle and blade mass (tons)	56.8, 240, 17.7	90, 285, 35	105.5, 446, 41.7

Table B.2
Model comparison of existing FOWTs controllers.

Model	Nature	DOFs	Incorporates incident wind/wave in controller synthesis
Jonkman [128]	Flexible 3-D	22/24	Wind only
Betti [140]	Rigid 2-D	7	Wind and Wave
Sandner [68]	Flexible 3-D	18	Wind and Wave
Homer [57]	Rigid 3-D	15/16	Wind and Wave

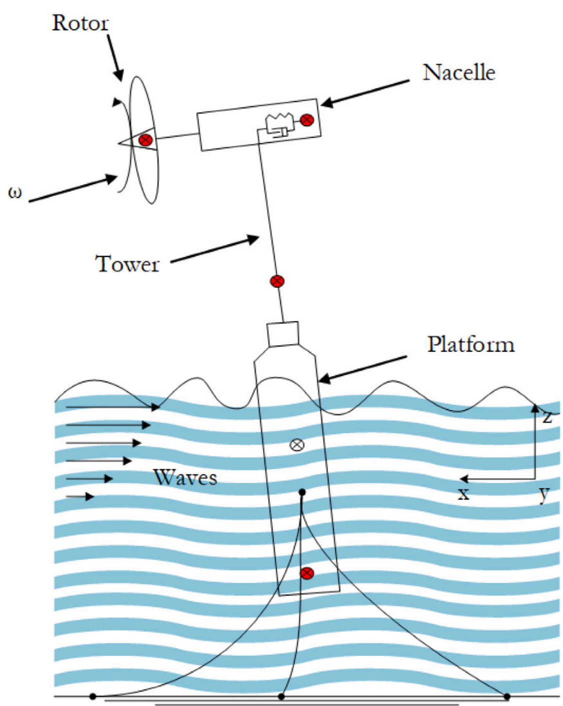

Fig. B.2. Adapted layout of Sander model [68].

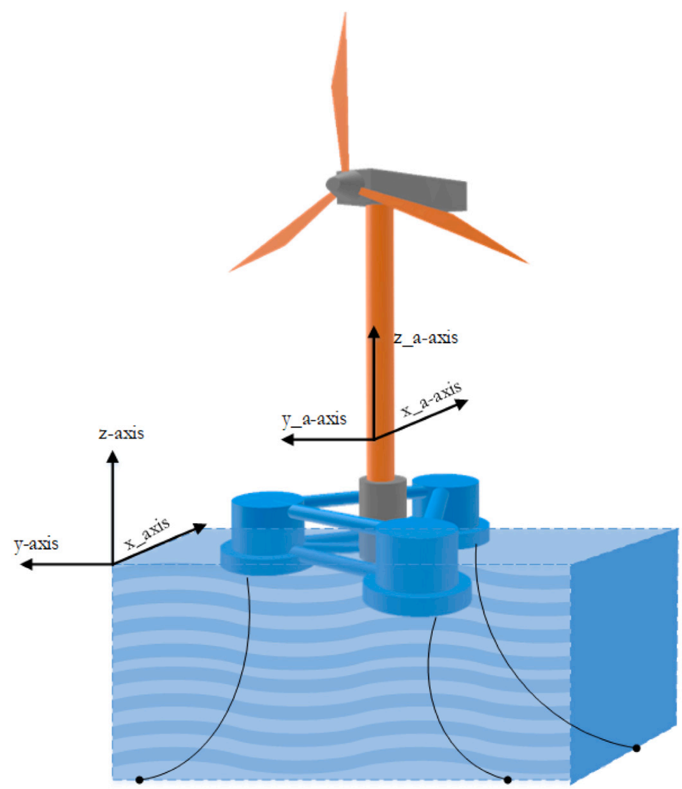

Fig. B.3. Adapted layout of Hommer model.

Betti model. To address the complexity of the existing simulation models for the FOWTs, a simplistic control-oriented 2-D rigid model is proposed by Betti et al. [140]. Betti model is designed with 7 states, where the incident wind and wave disturbances are considered acting in 2-D plane. The schematic of this model is given in Fig. B.1. This model may also generate linearized models at various locations within the operating domain. Unlike FAST, this model may also be used to calculate the wave disturbance matrix, which provides the incident wave information into the advanced control design process. The Betti model is used for the controller synthesis on a TLP based 5 MW FOWT considering 2-D incident disturbances. However, it was found that the model had a small effect on the platform motions and generated power despite the accurate 2-D motion representation [137,140].

Sander model. Sandner et al. [68] proposed a reduced FOWT model for a spar buoy platform as shown in Fig. B.2. The states of this model includes platform motion, rotor speed, nacelle movement, and pitching angle of the blades. The Sander model has a 2-D structure similar to Betti model [140] and its performance is found accurate when compared with the complex FAST model. However, Sander model may not be suitable to study FOWT based on other platforms because it is designed for a spar boy platform, where there is less hydrodynamic complexity involved due to its unique geometry. Moreover, Sandner model is only used for the 2-D disturbances, and its effectiveness in a 3-D scenario is yet to be assessed.

Homer model. Homer et al. [57] proposed a simple but effective control-oriented 3-D design for advanced control synthesis of a FOWT, as shown in Fig. B.3. Like other similar models, the Homer model also has fewer DOFs (15/16), and it may also be used to generate linearized models at a given operating point. The model is capable of reflecting 3-D motion, and assist controller synthesis to eliminate or reduce the effect of wind and wave disturbances. Furthermore, the Homer model also comes with an ability to generate wave disturbance matrix.

The simplified models are compared with complex model FAST in terms of their particular characteristics in Table B.2.

References

[1] GWEC GWEC. Global offshore wind report. 2020.
[2] Darwish AS, Al-Dabbagh R. Wind energy state of the art: present and future technology advancements. Renew Energy Environ Sustain 2020;5:7.
[3] Kaldellis JK, Kapsali M. Shifting towards offshore wind energy—Recent activity and future development. Energy Policy 2013;53:136–48.
[4] Wang J, Qin S, Jin S, Wu J. Estimation methods review and analysis of offshore extreme wind speeds and wind energy resources. Renew Sustain Energy Rev 2015;42:26–42.
[5] Wind Europe. Floating offshore wind vision statement. Tech. rep. June, 2017, p. 16.
[6] IPPC. Global warming of 1.5 °C. 2018, https://www.ipcc.ch/sr15/.
[7] Borch K, Clausen N-E, Ellis G. Environmental and social impacts of wind energy. Tech. rep., Technical University of Denmark (DTU); 2014.
[8] Dai K, Bergot A, Liang C, Xiang WN, Huang Z. Environmental issues associated with wind energy - A review. Renew Energy 2015;75:911–21.
[9] Leung DY, Yang Y. Wind energy development and its environmental impact: A review. Renew Sustain Energy Rev 2012;16(1):1031–9.
[10] Lee J, Zhao F. GWEC global wind report. Tech. rep., 2020, p. 78.
[11] Joyce L, Feng Z. Global offshore wind report 2020. Tech. rep. August, 2020, p. 130.
[12] Duan L, Li Y. Progress of recent research and development in floating offshore wind turbines. Sci Sin Phys Mech Astron 2016;46(12):124703.
[13] Borg M, Collu M. Offshore floating vertical axis wind turbines, dynamics modelling state of the art. Part III: Hydrodynamics and coupled modelling approaches. Renew Sustain Energy Rev 2015;46:296–310.
[14] Yu Y, Li Y. Preliminary results of a RANS simulation for a floating point absorber wave energy system under extreme wave conditions. Tech. rep., Golden, CO (United States): National Renewable Energy Lab.(NREL); 2011.
[15] Chen X, Jiang Z, Li Q, Li Y, Ren N. Extended environmental contour methods for long-term extreme response analysis of offshore wind turbines. J Offshore Mech Arct Eng 2020;142(5):052003.
[16] Ren Z, Verma AS, Li Y, Teuwen JJ, Jiang Z. Offshore wind turbine operations and maintenance: A state-of-the-art review. Renew Sustain Energy Rev 2021;144:110886.
[17] Li Y, Lence BJ, Calisal SM. An integrated model for estimating energy cost of a tidal current turbine farm. Energy Convers Manage 2011;52(3):1677–87.
[18] LaBonte A, O'Connor P, Fitzpatrick C, Hallett K, Li Y. Standardized cost and performance reporting for marine and hydrokinetic technologies. In: Proceedings of the 1st marine energy technology symposium (METS13). Washington, DC, USA; 2013. p. 10–11.
[19] Larsen TJ, Hanson TD. A method to avoid negative damped low frequent tower vibrations for a floating, pitch controlled wind turbine. J Phys Conf Ser 2007;75(1):012073.
[20] Jonkman JM. Dynamics modeling and loads analysis of an offshore floating wind turbine [Ph.D. thesis]. National Renewable Energy Laboratory; 2007.
[21] Lackner MA. Controlling platform motions and reducing blade loads for floating wind turbines. Wind Eng. 2009;33(6):541–54.
[22] Skaare B, Hanson TD, Nielsen FG. Importance of control strategies on fatigue life of floating wind turbines. In: 26th international conference on offshore mechanics and arctic engineering. San Diego, California; 2007. p. 1–8.
[23] Namik H, Stol K. Individual blade pitch control of floating offshore wind turbines. Wind Energy 2010;13(1):74–85.
[24] Namik H, Stol K. Individual blade pitch control of a spar-buoy floating wind turbine. IEEE Trans Control Syst Technol 2014;22(1):214–23.
[25] Namik H, Stol K. Performance analysis of individual blade pitch control of offshore wind turbines on two floating platforms. Mechatronics 2011;21(4):691–703.
[26] Bagherieh O, Nagamune R. Gain-scheduling control of a floating offshore wind turbine above rated wind speed. Control Theory Technol 2015;13(2):160–72.
[27] Schlipf D, Sandner F, Raach S, Matha D, Cheng PW. Nonlinear model predictive control of floating wind turbines. In: The twenty-third (2013) international offshore and polar engineering. Anchorage, Alaska, USA; 2013. p. 440–46.
[28] Raach S, Schlipf D, Sandner F, Matha D, Cheng PW. Nonlinear model predictive control of floating wind turbines with individual pitch control. In: Proceedings of the American control conference. Portland, Oregon, USA; 2014. p. 4434–39.
[29] Lemmer F, Raach S, Schlipf D, Cheng PW. Prospects of linear model predictive control on a 10MW floating wind turbine. In: The ASME 2015 34th international conference on ocean, offshore and arctic engineering. 2015. p. 1–11.
[30] Navalkar ST, van Wingerden J-W, Fleming PA, van Kuik GAM. Integrating robust lidar-based feedforward with feedback control to enhance speed regulation of floating wind turbines. In: American Control Conference. IEEE; 2015, p. 3070–5.
[31] Schlipf D, Simley E, Lemmer F, Pao L, Cheng PW. Collective pitch feedforward control of floating wind turbines using lidar. In: Twenty-fifth (2015) international ocean and polar engineering conference. vol. 2. Kona, Big Island, Hawaii; 2015. p. 324–31.
[32] Li Y, Çalisal SM. Numerical simulation of ship maneuverability in wind and current, with escort tugs. Mar Technol Sname News 2005;42(04):159–76.
[33] Xia Y, Xu K, Li Y, Xu G, Xiang X. Improved line-of-sight trajectory tracking control of under-actuated AUV subjects to ocean currents and input saturation. Ocean Eng 2019;174:14–30.
[34] Xia Y, Xu K, Li Y, Xu G, Xiang X. Adaptive trajectory tracking control of a cable-driven underwater vehicle on a tension leg platform. IEEE Access 2019;7:35512–31.
[35] Yi J-H, Yoon G-L, Li Y. Numerical investigation on effects of rotor control strategy and wind data on optimal wind turbine blade shape. Wind Struct 2014;18(2):195–213.
[36] Lackner MA, Rotea MA. Structural control of floating wind turbines. Mechatronics 2011;21(4):704–19.
[37] Harsh S Dhiman. Machine learning in wind forecasting. 2020.
[38] Karasu S, Altan A, Saraç Z, Hacioğlu R. Prediction of wind speed with non-linear autoregressive (NAR) neural networks. In: 2017 25th Signal Processing and Communications Applications Conference (SIU). IEEE; 2017, p. 1–4.
[39] Altan A, Karasu S, Zio E. A new hybrid model for wind speed forecasting combining long short-term memory neural network, decomposition methods and grey wolf optimizer. Appl Soft Comput 2021;100:106996.
[40] Li Y, Colby JA, Kelley N, Thresher R, Jonkman B, Hughes S. Inflow measurement in a tidal strait for deploying tidal current turbines: Lessons, opportunities and challenges. In: International conference on offshore mechanics and arctic engineering, vol. 49118. p. 569–76.
[41] Li L, Yuan Z, Gao Y, Zhang X. Wave force prediction effect on the energy absorption of a wave energy converter with real-time control. IEEE Trans Sustain Energy 2018;10(2):615–24.
[42] Li L, Gao Y, Ning DZ, Yuan ZM. Development of a constraint non-causal wave energy control algorithm based on artificial intelligence. Renew Sustain Energy Rev 2020;110519.
[43] Schlink U, Tetzlaff G. Wind speed forecasting from 1 to 30 minutes. Theor Appl Climatol 1998;60(1):191–8.
[44] Torres JL, Garcia A, De Blas M, De Francisco A. Forecast of hourly average wind speed with ARMA models in navarre (Spain). Sol Energy 2005;79(1):65–77.
[45] Sfetsos A. A novel approach for the forecasting of mean hourly wind speed time series. Renew Energy 2002;27(2):163–74.
[46] Kavasseri RG, Seetharaman K. Day-ahead wind speed forecasting using f-ARIMA models. Renew Energy 2009;34(5):1388–93.
[47] Ait Maatallah O, Achuthan A, Janoyan K, Marzocca P. Recursive wind speed forecasting based on Hammerstein auto-regressive model. Appl Energy 2015;145:191–7.
[48] Dunne F, Pao LY, Schlipf D, Scholbrock AK. Importance of lidar measurement timing accuracy for wind turbine control *. In: 2014 American control conference. American Automatic Control Council; 2014, p. 3716–21.
[49] Schlipf D, Schlipf DJ, Kühn M. Nonlinear model predictive control of wind turbines using LIDAR. Wind Energy 2013;16(2013):1107–29.
[50] NOAA Ocean Explorer: Types of offshore oil and gas structures, http://appliedmechanicsreviews.asmedigitalcollection.asme.org/article.aspx?doi=10.1115/1.4031175.
[51] Wu X, Hu Y, Li Y, Yang J, Duan L, Wang T, et al. Foundations of offshore wind turbines: A review. Renew Sustain Energy Rev 2019;104:379–93.
[52] Henderson AR, Witcher D. Floating offshore wind energy - A review of the current status and an assessment of the prospects. Wind Eng 2010;34(1):1–16.
[53] Samani AE, de Kooning JD, Kayedpour N, Singh N, Vandevelde L. The impact of pitch-to-stall and pitch-to-feather control on the structural loads and the pitch mechanism of a wind turbine. Energies 2020;13(17).
[54] Skaare B, Hanson TD, Nielsen FG, Yttervik R, Hansen AM. Integrated dynamic analysis of floating offshore wind turbines. In: European wind energy conf. and exhibition. Milan, Italy; 2007.
[55] Jonkman J, Butterfield S, Musial W, Scott G. Definition of a 5-MW reference wind turbine for offshore system development. Tech. rep. February, National Renewable Energy Laboratory; 2009, p. 75.
[56] Matha D. Model development and load analysis of an offshore wind turbine. Tech. rep., University of Colorado - Boulder; 2010, p. 1–129.
[57] Homer JR, Nagamune R. Physics-based 3-D control-oriented modeling of floating wind turbines. IEEE Trans Control Syst Technol 2018;26(1):14–26.
[58] Cortes Sanchez CJ. Wind and wave disturbance rejection control of floating offshore wind turbines [Master's thesis]. 2018.
[59] Lemmer F, Schlipf D, Cheng PW. Control design methods for floating wind turbines for optimal disturbance rejection. In: Journal of physics: Conference series. vol. 753, 2016. p. 092006.
[60] Lemmer F, Raach S, Schlipf D, Cheng PW. Parametric wave excitation model for floating wind turbines. In: 13th deep sea offshore wind R&D conference, EERA DeepWind'2016, 20-22 January 2016, vol. 94. 2016. p. 290–305.
[61] Bakka T, Karimi HR, Duffie NA. Gain scheduling for output H∞ control of offshore wind turbine. In: Twenty-second (2012) international offshore and polar engineering conference. Rhodes, Greece; 2012. p. 496–501.
[62] Bagherieh O, Hedrick K, Horowitz R. Nonlinear control of floating offshore wind turbines using input/output feedback linearization and sliding control. In: Asme dynamic systems & control conference. 2014. p. 10.
[63] Zhao P, Nagamune R. Switching LPV control of a floating offshore wind turbine on a semi-submersible platform. In: IEEE international symposium on industrial electronics. IEEE; 2019, p. 664–9.

[64] Schlipf D, Schlipf DJ, Kühn M. Nonlinear model predictive control of wind turbines using LIDAR. Wind Energy 2013;16(7):1107–29.

[65] Schuurmans J, Nederkoorn E, Kanev S, Rutteman R, Nguyen E. Optimised aerodynamics and control by nonlinear model based predictive control. In: European wind energy association conference. 2013. p. 1–9.

[66] Körber A, King R. Model predictive control for wind turbines. In: Proc. of European wind energy conference. 2010. p. 1–7.

[67] Schlipf D, Fleming P, Haizmann F, Scholbrock A, Hofsäß M, Wright A, Cheng PW. Field testing of feedforward collective pitch control on the cart2 using a nacelle-based lidar scanner. J Phys: Conf Ser 2014;555(1):012090.

[68] Sandner F, Schlipf D, Matha D, Seifried R, Cheng PW. Reduced nonlinear model of a spar-mounted floating wind turbine. In: Proceedings of the German wind energy conference (DEWEK). Bremen, Germany; 2012. p. 4.

[69] Bossanyi EA, Kumar A, Hugues-Salas O. Wind turbine control applications of turbine-mounted LIDAR. J Phys Conf Ser 2014;555(1):12011.

[70] Dunne F, Pao LY, Wright AD, Jonkman B, Kelley N. Adding feedforward blade pitch control to standard feedback controllers for load mitigation in wind turbines. Mechatronics 2011;21(4):682–90.

[71] Schlipf D, Schuler S, Grau P, Martin K. Look-ahead cyclic pitch control using LIDAR. In: The science of making torque from wind. Greece; 2010. p. 1–7.

[72] Mikkelsen T. Lidar-based research and innovation at DTU wind energy – A review. J Phys Conf Ser 2014;524(1):012007.

[73] Dunne F, Pao L, Wright A, Jonkman B, Kelley N. Combining standard feedback controllers with feedforward blade pitch control for load mitigation in wind turbines. In: 48th AIAA aerospace sciences meeting including the new horizons forum and aerospace exposition. Orlando, Florida; 2010. p. 18.

[74] Spencer BF, Sain MK. Controlling buildings: A new frontier in feedback. Shock Vib Dig 1998;30(4):267–81.

[75] Li H, Jing X, Karimi HR. Output-feedback-based H∞ control for vehicle suspension systems with control delay. IEEE Trans Ind Electron 2014;61(1):436–46.

[76] He W, Zhang S, Ge SS. Adaptive control of a flexible crane system with the boundary output constraint. IEEE Trans Ind Electron 2014;61(8):4126–33.

[77] Li H, Yu J, Hilton C, Liu H. Adaptive sliding-mode control for nonlinear active suspension vehicle systems using T–S fuzzy approach. IEEE Trans Ind Electron 2013;60(8):3328–38.

[78] Spencer Jr BF, Nagarajaiah S. State of the art of structural control. J Struct Eng 2003;129(7):845–56.

[79] Namik H, Rotea M, Lackner M. Active structural control with actuator dynamics on a floating wind turbine. In: American institute of aeronautics and astronautics, new horizons forum and aerospace exposition. January. 2013. p. 1–16.

[80] Stewart G, Lackner M. Offshore wind turbine load reduction employing optimal passive tuned mass damping systems. IEEE Trans Control Syst Technol 2013;21(4):1090–104.

[81] Tsouroukdissian AR, Park S, Pourazarm P, Cava WL, Lackner M, Lee S, et al. Smart novel semi-active tuned mass damper for fixed-bottom and floating offshore wind. In: Offshore technology conference. 2016. p. 1–17.

[82] Li X, Gao H. Load mitigation for a floating wind turbine via generalized H∞ structural control. IEEE Trans Ind Electron 2016;63(1):332–42.

[83] Ha M, Cheong C. Pitch motion mitigation of spar-type floating substructure for offshore wind turbine using multilayer tuned liquid damper. Ocean Eng 2016;116:157–64.

[84] Hu Y, Chen MZQ. Passive structural control with inerters for a floating offshore wind turbine. In: 36th Chinese control conference. 2017. p. 9266–71.

[85] Li Y, Wu Z. Stabilization of floating offshore wind turbines by artificial muscle based active mooring line force control. In: Proceedings of the American control conference. 2016. p. 2277–82.

[86] Dhiman HS, Deb D. A review of wind speed and wind power forecasting techniques, arxiv. 2020.

[87] Gneiting T, Larson K, Westrick K, Genton MG, Aldrich E. Calibrated probabilistic forecasting at the stateline wind energy center. J Amer Statist Assoc 2006;101(475):968–79.

[88] Guo Z-h, Wu J, Lu H-y, Wang J-z. A case study on a hybrid wind speed forecasting method using BP neural network. Knowl-Based Syst 2011;24(7):1048–56.

[89] Li G, Shi J. On comparing three artificial neural networks for wind speed forecasting. Appl Energy 2010;87(7):2313–20.

[90] Barbounis TG, Theocharis JB. Locally recurrent neural networks for long-term wind speed and power prediction. Neurocomputing 2006;69(4–6):466–96.

[91] Mohandes MA, Halawani TO, Rehman S, Hussain AA. Support vector machines for wind speed prediction. Renew Energy 2004;29(6):939–47.

[92] Gani A, Mohammadi K, Shamshirband S, Altameem TA, Petković D. A combined method to estimate wind speed distribution based on integrating the support vector machine with firefly algorithm. Environ Prog Sustain Energy 2016;35(3):867–75.

[93] Zhou J, Shi J, Li G. Fine tuning support vector machines for short-term wind speed forecasting. Energy Convers Manage 2011;52(4):1990–8.

[94] Petković D, Shamshirband S, Anuar NB, Saboohi H, Wahab AWA, Protić M, et al. An appraisal of wind speed distribution prediction by soft computing methodologies: A comparative study. Energy Convers Manage 2014;84:133–9.

[95] Mori H, Kurata E. Application of gaussian process to wind speed forecasting for wind power generation. In: 2008 IEEE international conference on sustainable energy technologies, ICSET 2008. IEEE; 2008, p. 956–9.

[96] Li G, Shi J. Applications of Bayesian methods in wind energy conversion systems. Renew Energy 2012;43:1–8.

[97] Liu H, Tian H-q, Li Y-f. Four wind speed multi-step forecasting models using extreme learning machines and signal decomposing algorithms. Energy Convers Manage 2015;100:16–22.

[98] Guo Z, Zhao W, Lu H, Wang J. Multi-step forecasting for wind speed using a modified EMD-based artificial neural network model. Renew Energy 2012;37(1):241–9.

[99] Nikolić V, Motamedi S, Shamshirband S, Petković D, Ch S, Arif M. Extreme learning machine approach for sensorless wind speed estimation. Mechatronics 2016;34:78–83.

[100] Shamshirband S, Mohammadi K, Tong CW, Petković D, Porcu E, Mostafaeipour A, et al. Application of extreme learning machine for estimation of wind speed distribution. Clim Dynam 2016;46(5–6):1893–907.

[101] Cadenas E, Rivera W. Wind speed forecasting in three different regions of Mexico, using a hybrid ARIMA–ANN model. Renew Energy 2010;35(12):2732–8.

[102] Wang J, Hu J, Ma K, Zhang Y. A self-adaptive hybrid approach for wind speed forecasting. Renew Energy 2015;78:374–85.

[103] Simley E, Pao L, Frehlich R, Jonkman B, Kelley N. Analysis of wind speed measurements using continuous wave LIDAR for wind turbine control. In: 49th AIAA aerospace sciences meeting including the new horizons forum and aerospace exposition. 2011. p. 263.

[104] Valldecabres L, Peña A, Courtney M, von Bremen L, Kühn M. Very short-term forecast of near-coastal flow using scanning lidars. Wind Energy Sci 2018;3(1):313–27.

[105] Simon E, Courtney M, Vasiljevic N. Minute-scale wind speed forecasting using scanning lidar inflow measurements. Wind Energy Sci Discuss 2018;1–30.

[106] WAVEWATCH III (WW3), https://polar.ncep.noaa.gov/waves/wavewatch/.

[107] Forecasts — ECMWF, https://www.ecmwf.int/en/forecasts.

[108] SWAN, https://www.tudelft.nl/citg/over-faculteit/afdelingen/hydraulic-engineering/sections/environmental-fluid-mechanics/research/swan.

[109] Fusco F, Ringwood JV. Short-term wave forecasting for real-time control of wave energy converters. IEEE Trans Sustain Energy 2010;1(2):99–106.

[110] Pena Sanchez Y, Ringwood J. A critical comparison of AR and ARMA models for short-term wave forecasting. In: Proceedings of the twelfth European wave and tidal energy conference. 2017. p. 9611–16.

[111] Ge M, Kerrigan EC. Short-term ocean wave forecasting using an autoregressive moving average model. In: 2016 UKACC 11th international conference on control (CONTROL). IEEE; 2016, p. 1–6.

[112] Deo MC, Naidu CS. Real time wave forecasting using neural networks. Ocean Eng 1998;26(3):191–203.

[113] Sadeghifar T, Nouri Motlagh M, Torabi Azad M, Mohammad Mahdizadeh M. Coastal wave height prediction using Recurrent Neural Networks (RNNs) in the south Caspian Sea. Mar. Geod 2017;40(6):454–65.

[114] Ni C, Ma X, Bai Y. Convolutional neural network based power generation prediction of wave energy converter. In: 2018 24th international conference on automation and computing (ICAC). IEEE; 2018, p. 1–6.

[115] Akpınar A, Özger M, Kömürcü MI. Prediction of wave parameters by using fuzzy inference system and the parametric models along the south coasts of the black sea. J Mar Sci Technol 2014;19(1):1–14.

[116] Wu M, Stefanakos C, Gao Z, Haver S. Prediction of short-term wind and wave conditions for marine operations using a multi-step-ahead decomposition-ANFIS model and quantification of its uncertainty. Ocean Eng 2019;188:106300.

[117] Reikard G, Pinson P, Bidlot J-R. Forecasting ocean wave energy: The ECMWF wave model and time series methods. Ocean Eng 2011;38(10):1089–99.

[118] Woodcock F, Engel C. Operational consensus forecasts. Weather Forecast 2005;20(1):101–11.

[119] Woodcock F, Greenslade DJM. Consensus of numerical model forecasts of significant wave heights. Weather Forecast 2007;22(4):792–803.

[120] Ma Y, Sclavounos PD, Cross-Whiter J, Arora D. Wave forecast and its application to the optimal control of offshore floating wind turbine for load mitigation. Renew Energy 2018;128:163–76.

[121] Hou ZS, Wang Z. From model-based control to data-driven control: Survey, classification and perspective. Inform Sci 2013;235:3–35.

[122] Brunton SL, Noack BR. Closed-loop turbulence control: Progress and challenges. Appl Mech Rev 2015;67(5):050801.

[123] Kane MB. Machine learning control for floating offshore wind turbine individual blade pitch control. In: Proceedings of the American control conference 2020-July. 2020. p. 237–41.

[124] Schmid PJ. Dynamic mode decomposition of numerical and experimental data. J Fluid Mech 2010;656:5–28.

[125] Brunton SL, Proctor JL, Kutz JN. Discovering governing equations from data by sparse identification of nonlinear dynamical systems. Proc Natl Acad Sci 2016;113(15):3932–7.

[126] Proctor JL, Brunton SL, Kutz JN. Generalizing Koopman theory to allow for inputs and control. SIAM J Appl Dyn Syst 2018;17(1):909–30.

[127] Betz A. Introduction to the theory of flow machines. 1966, 5–6.
[128] Jonkman JM, Jr MLB. FAST user's guide. Tech. rep., National Renewable Energy Laboratory; 2005.
[129] Malcolm DJ, Hansen AC. WindPACT turbine rotor design study, vol. 5. Golden, CO: National Renewable Energy Laboratory; 2002.
[130] Recommendations for design of offshore wind turbines (RECOFF), https://cordis.europa.eu/project/id/ENK5-CT-2000-00322.
[131] Goezinne F. Terms of reference DOWEC. Bunnik: NEG-Micon; 2001.
[132] Larsen TJ, Hansen AM. How 2 HAWC2, the user's manual. Risø National Laboratory; 2007.
[133] Bak C, Zahle F, Bitsche R, Kim T, Yde A, Henriksen LC, et al. The DTU 10-MW reference wind turbine. In: Danish wind power research, Fredericia, Denmark. 2013.
[134] Wind turbine design software — Bladed - DNV GL, https://www.dnvgl.com/services/wind-turbine-design-software-bladed-3775.
[135] LEANWIND http://www.leanwind.eu/.
[136] Desmond C, Murphy J, Blonk L, Haans W. Description of an 8 MW reference wind turbine. In: Journal of physics: Conference series. vol. 753. 2016.
[137] Betti G, Farina M, Guagliardi GA, Marzorati A, Scattolini R. Development of a control-oriented model of floating wind turbines. IEEE Trans Control Syst Technol 2014;22(1):69–82.
[138] SIMPACK MBS Software — Wind, http://www.simpack.com/industrial_sectors_wind.html.
[139] Matha D, Beyer F. Offshore wind turbine hydrodynamics modelling in SIMPACK. SIMPACK News 2013. July.
[140] Betti G, Farina M, Marzorati A, Scattolini R, Guagliardi GA. Modeling and control of a floating wind turbine with spar buoy platform. In: 2nd IEEE international energy conference and exhibition, ENERGYCON 2012. 2012. p. 189–94.